

Manuscript Number: PALAE07293R1

Title: Miocene-Pliocene rocky shores on São Nicolau (Cape Verde Islands): Contrasting windward and leeward biofacies on a volcanically active oceanic island

Article Type: Research Paper

Keywords: Coastal deposition, Miocene, Pliocene, Rhodoliths (Rhodophyta), Northeast Trade Winds, Volcanic islands

Corresponding Author: Dr. Markes E. Johnson, PhD

Corresponding Author's Institution: Williams College

First Author: Markes E. Johnson, PhD

Order of Authors: Markes E. Johnson, PhD; Ricardo S Ramalho, PhD; B Gudveig Baarli, PhD; Mário Cachao, PhD; Carlos M Silva, da, M Sci.; Eduardo J Mayoral, PhD; Ana Santos, PhD

Abstract: North Atlantic islands in the Cape Verde Archipelago off the coast of West Africa commonly feature an elongated N-S shape in which reduced northern coasts and longer eastern shores absorb the brunt of wave activity and long-shore currents generated by prevailing North East Trade Winds. Located in the middle windward islands, São Nicolau is unusual in profile with an elongated E-W configuration that offers a broad target against high-energy, wind-driven waves. Conversely, the south shore of São Nicolau provides relatively wide shelter in a leeward setting. Reconstruction of the proto-island prior to the onset of the Main Eruptive stage during the Late Miocene at ~5.1 Ma reveals a moderately smaller island with essentially the same E-W orientation. This study combines previous data with results from a detailed stratigraphic log based on Upper Miocene limestone deposits on the island's south flank for comparison with stratigraphic profiles of Upper Miocene limestone from the island's northeast quarter. Logs from a Pliocene sandy limestone outcropping on the south-central coast of São Nicolau give added context to the diversity of marine invertebrates, including branching coral colonies and delicate ramose bryozoans that found shelter in a leeward setting. Whole rhodoliths contribute the main fabric of carbonates deposited against rocky shores on the northern, exposed side of the Miocene island, whereas only traces of worn rhodoliths and rhodolith sand occur as in finer Miocene grainstone on the island's southern, protected side. Miocene and Pliocene carbonate deposits were terminated by submarine flows on an actively growing volcanic island. The passage zone from submarine to subaerial flows on the island's flanks makes a useful meter-stick to gauge absolute water depth at the moment of local extinction by volcanic activity.

## REVISION NOTES (for manuscript PALAEO7293)

We received the reviews for this manuscript on October 4, 2013 with a recommendation for major revision. After discussion among the co-authors, it was agreed that a significant part of the revision must feature two important elements: 1) a new stratigraphic log from the leeward, southeast side of the Cape Verdean island of São Nicolau, and 2) new thin sections of the fossil rhodoliths from our collections to determine the floral identity at least to genus level. In particular, one of the recommendations from Reviewer #2 was to incorporate a reference by Braga et al. (2010) outlining a distinction among different living and fossil coralline red algae that form as rhodoliths regulated by the original water depth. Identification of the Miocene rhodoliths from our stratigraphic profiles now adds a critical element to the story that serves to test the concept of depth relationships in fossil rhodoliths.

The earlier version of our paper included comments under section 2.3 (Previous paleontological studies) giving general observations on Miocene strata from the south side of São Nicolau not formalized in detail with a proper stratigraphic log. That part of the island is difficult to reach and only one member of our team had visited the place prior to our project. Our treatment of these incomplete data confused Reviewer #2, who inquired with a notation on line 525 of the original submission: “Where is the fossil content described in terms of paleobathymetry?” Also, in line 565, where it is asked whether a conclusion comes from the literature or an original observation by our team. Thus, one of our goals for the revised ms. was to provide the detailed stratigraphic log for a locality at Baía dos Barreiros (new Fig. 6). In order to do this, a member of our team (RSR) returned to São Nicolau in October/November to compile the data from this locality. Thus, we now submit a manuscript with a total of nine figures, an increase by one to accommodate the new profile from Baía dos Barreiros.

In the following commentary, we respond to the comments and suggestions offered by the journal’s editor, Reviewer #1, and Reviewer #2. Original commentary is shown in black and our response is shown in red.

Editor’s notes

All items specifically listed by the editor for correction have been complied with and corrected in the revised manuscript. Only one comment asked for modification of a particular figure:

Fig. 1: Please indicate latitudes and longitudes on map in upper right.

**Done.** Note that additional lines of latitude and longitude are already shown in the larger map for São Nicolau provided in Fig. 2.

## Reviewer #1

The present paper is a good contribution and I find very informative and well organized. I feel the paper have a very long results section but I feel this need to be reflected in the discussion where I think there are no implications of the rhodolith sphericity data or other implications of their findings about rhodolith material.

NOTE: There is a contradiction between the editor's request for a shorter discussion and Reviewer #1 asking for the results to be better treated in the discussion. New results describing the stratigraphic log from Baía dos Barreiros have been added (lines 304-321). More to the point of the comment by Reviewer #1, a new section under the discussion (5.2 Composition and morphodynamics of São Nicolau rhodoliths) has been added (see lines 444-468). This addition is compensated for by removal of a large part of the discussion that reviewed information from published papers on other paleoislands (see excised lines 471-495).

## Reviewer #2

The text is concise and well written. The stratigraphic and sedimentary data are well analysed and the illustrations represent a detailed account of the analysed stratigraphic sequences. **So positive!**

However, the readers would be greatly helped in understanding the studied scenario if a clear and detailed windward and leeward biotas are described and distinguished (even with tables). Rhodoliths are quoted in the highlights and in the abstract but a detailed description of the rhodolith assemblages is missing. The triangular diagrams do not really show a clear contrast among the rhodolith assemblages as stated in the highlights.

In terms of rhodoliths, there is largely one kind of assemblage – a transported assemblage – while some other details associated with the substrate indicate an *in situ* biota (trace fossils as borings). The faunal composition is quite simple and we don't believe that tables are the answer to this situation. Instead, we supply a more forceful statement regarding the differences between *in situ* and transported assemblages on both leeward and windward sides of the island.

The reviewer fails to understand the significance of the triangular plots that show extreme roundness. Possibly, there is a misunderstanding about these plots, thinking that some are for specimens from a windward setting as opposed to others from a leeward setting – when in fact all come from the windward side of the island. Allusion to naming things in tables also implies that the reviewer is looking for identification of the rhodoliths by genus and species. Using the new thin sections, we have accomplished this at the genus level. Only a single genus can be identified from our thin sections. We have returned to the thin-section studies published by

Torres and Soares (1946) that confirm *Lithothamnium* as the only genus so far identified with respect to rhodoliths from the island of São Nicolau. The paper by Braga et al. (2010) recommended to us by Reviewer #2 makes a compelling argument that many fossil identifications of rhodoliths to species level are unreliable. Thus, we feel comfortable keeping our identification at the genus level.

I find a number of problems with the presentation of the science (regarding the biotic content and the palaeoecological discussion/interpretation) and at this stage I would recommend its publication after major revision. **Intensely negative!** It should be returned to the authors for consideration for major revision with to the palaeoecology of the Upper Miocene-Pliocene marine assemblages. Nonetheless, the manuscript could be limited to deal with the stratigraphic and geological data. If this would be the case the authors should leave out the statements to the biogenic components of the limestone which are not really facies analysed in detail.

**NOTE:** We have adopted the suggestion by Reviewer #2 to emphasis the stratigraphic and geological data over “species” data in our revision. Thus, we consistently refer to biofacies mainly in a sedimentological sense – as opposed to species-level identifications. Comparison with living marine fauna is beyond the scope of this paper, because adequate biological work remains to be done in the Cape Verde islands.

I have added several comments and suggestions into the text (line commentary).

**NOTE:** It is *only* in the commentary addressed to specific lines in our manuscript that the reviewer’s objections are hinted at.

Line 46 (Keywords): Rhodoliths – These are not really treated in detail in the study

**Taxonomic considerations are now a part of this study, particularly in response to the paper by Braga et al. (2010), but only at a genus level for the rhodoliths.**

Line 81: The paper by Halfor & Mutti (2005) is an over simplification of the rhodolith distribution in the fossil record. There are several examples that show thick Oligocene rhodolith deposits (see Braga et al., 2010).

**NOTE:** Halfor & Mutti (2005) are cited in the paper by Braga et al., (2010) with only a slight adjustment suggesting that maximum diversification occurred during the Early Miocene as opposed to the Middle Miocene. Furthermore, the Braga paper takes a particularly strong stand by arguing that the many species names for fossil rhodoliths currently in use are unreliable. This puts into question any attempt to determine the maximum time interval of rhodolith species diversity! **HOWEVER**, we can accept Braga’s determination of an Early Miocene high.

Line 102: The “differences in biotas” are not really explored in detail in their study. It would need at least a table for comparisons between the fossil assemblages and the possible present-day counter parts.

Because the fauna differences are so striking, while at the same time involving so few “species” – tables are unnecessary. The strat columns are sufficient for this purpose. ALSO, with the visit by coauthor RSR to the locality at Baía do Barreiros – we are now able to add another stratigraphic section (Fig. 6) to emphasize the absence of whole rhodoliths on the south side of the island.

Line 151: interpreted – By means of what? This is in reference to the paper by Bernoulli et al (2007), where the age is interpreted on the basis of micro-fossils.

Line 248: attributed – Why attributed? Have you not checked the main building organisms? We substitute the word “assigned” for attributed and state that we have visited the locality and are able to confirm the main biogenic component.

Line 274: Subsection 4.3 on Fossil rhodolith shape analysis – The data of these analyses are not successively discussed and interpreted.

As per recommendation of Reviewer #1, we now include a section that further deals with these analyses under section 5.2. There (lines 447-448), we emphasize that limitation to the upper point of the triangle is among the most extreme we have ever found in both our own analyses and those of many other authors. It is as if the reviewer believes we are hiding data regarding other rhodoliths with other shapes. There are no other shapes to discuss in terms of the material available.

Lines 289-290: This is an interpretation and should be moved to the Discussion. OK

Line 297: former palaeoshore – How do you know the relationship with the former palaeoshore? Do you guess it from stratigraphic correlation or are there hints from the fossil content?

This is based on close physical relationship to basal substrate in addition to the changing nature of the faunal content -- and this is clearly shown in Fig. 2.

Lines 382-386: on reaching relatively high-energy conditions – Why? What are the evidences?

The preceding sentence clearly states the evidence.

Line 392: death assemblages – What are the evidences of this? This needs to be justified.

Living rhodoliths are rarely packed more than two deep. The reviewer does not seem to understand that we can keep track of the paleoshore by noting proximity to

the basement rocks and also by observing the presence or absence of basalt-rock cores within the rhodoliths. Rhodoliths stacked deep against a paleoshore cannot represent living conditions! Furthermore, the data supplied in the paper by Braga et al. (2010) makes no reference what so ever to thicknesses of rhodolith beds. Rather, it supports the concept that different species of rhodoliths live in deeper, more offshore waters in contrast to species that live in shallower, nearshore waters. This distinction is reviewed in our discussion section and it helps strengthen our arguments now that we know we are dealing exclusively with forms belong to the genus *Lithothamnion*.

Line 414: Dott (1974) – What are the possible relationships between this example and the case study?

The relevance is that other studies find evidence of generally thick basal conglomerates on one side of a paleoisland (windward setting), but with reduced clast sizes or not at all present on the opposite side (leeward setting). In the revised paper, we cite Dott (1974) only to show that continental islands have been described dating as far back as the Cambrian.

Line 462: Rong et al. (2013) - Same criticism, but the reference is now removed.

Lines 442-433: deprived of sunlight – Coralline red algae can survive for a long time without light. What are the evidences for such a statement? This means a relatively abrupt mass mortality.

Yes, we have ample evidence from coastal deposits on Fuerteventura in the Canary Islands that an abrupt mass mortality of rhodoliths can take place through storm deposits. We have added this comment based on our experience with such contemporary deposits (see line 449).

Line 444: encrusting corals – does this mean that the encrusting corals thrived when the coralline algae did not?

Correct ! This is obvious from the photo in the original article, because the coral makes a lop-sided counterweight that makes it impossible for the rhodolith to move. The rhodolith was immobile at the time of coral encrustation. The present article under consideration is not the place to rehash information readily accessible in the published literature.

Line 452: whereas – There should be differences in the coralline taxonomic assemblages. No mention of this?

We have added information on the fossil genus identifications from the Hill of Oranges and Pedra de Agua localities on Ilhéu de Cima (Porto Santo, Madeira Archipelago) in the Madeira islands. In this particular case, the results only partially support the predictions of Braga et al. (2010).

Line 525: agree reasonable well with fossil content – Where is the fossil content described and interpreted in terms of paleobathymetry? This needs a clear description in the text.

The insertion of new text related in Fig. 6 in the results and discussion sections resolves this issue.

Line 547: shallow, sub-tidal marine biotas – These three marine biotas are not clearly defined / described / circumscribed in the text.

This is from the Conclusions section! There now exists a fourth strat section (Fig. 6) based on the recent fieldwork. By RSR. Furthermore, this issue is adequately treated (and in a novel way) under section 5.4 dealing with the use of volcanic sequences to gauge absolute water depth.

Line 565: Conclusion 2 – Is this a conclusion achieved by the present paper – or is it from the literature? Is there any evidence of this from the coralline taxonomic assemblages (i.e. deep-water coralline assemblages) or re-sedimented shoreward?

This aspect is resolved by addition of the new stratigraphic log from Baía dos Barreiros (Fig. 6) and the confirmation that we are dealing with only a single genus of rhodoliths from the Miocene of São Nicolau.

Lines 567-568: Do you think this is due to paleoenvironmental reasons or to redeposition?

The red-algal fragments are due to redeposition and we have strengthened this argument through the addition of the new stratigraphic log from Baía de Barreiros (Fig. 6) and accompanying texts.

Line 586: no discrepancy indicated by fossil content – What fossil content would point out those water depths?

Citations related to trace fossils help reaffirm the depth measurements concluded from the overlying lava deltas.

Line 589: original water depth – This should be a more detailed discussion by comparison by fossil contents of the limestone. The fossil content should be described at a species level (or at least at genus level) in order to provide consistent comparisons with present-day counter parts.

New information on rhodolith genera is added and we re-emphasize other factors – such as the occurrence of very delicate bryozoans in the leeward setting.

Fig. 5: In the highlights, you state: “Shape analysis of abundant rhodoliths shows selection for transported forms.” This is not really evident in these diagrams where the dominating rhodoliths are spheroidal in shape. In a selected rhodolith assemblage, I would expect a more evident contrast between the shapes.

Again, the reviewer shows ignorance based on what the diagrams are intended to test and to show. If the reviewer is hoping to find differences in rhodoliths based on the premise of the Braga et al. (2010) paper, then he will be disappointed. We cannot add shapes to the triangular plots that do not exist. We have only one shape to exhibit and we re-emphasize that a kind of winnowing action is strongly implied.

### Summary

All corrections required by the journal’s editor have been made. Reviewer #1 offered only a brief report that chiefly asked for a better discussion on the repercussions of our shape analyses (Fig. 5) in the discussion section. This has been done. Reviewer #2 found our contribution to be concise and well written. However, he/she had many criticisms that were spelled out only by the many notations added in the margins of our text. We believe that we have answered each and every one of those criticisms. Clearly, Reviewer #2 has a high regard for the 2010 paper by Braga et al. That paper sets out certain predictions regarding the depth preferences of rhodoliths by genera. We have taken pains to add to our present manuscript new data on generic identifications from our collections from São Nicolau – as well as a summary of the generic identifications previously reported in some of our earlier studies on fossil rhodoliths from the Canary and Madeira islands. Some references marked by Reviewer #2 as superfluous have been removed from the text and bibliography. The submitted “Highlights” have been amended to better reflect the key aspects of our study related to transported assemblages. We hope that sufficient information is now at hand to reconsider our manuscript for publication in PPP.



1  
2  
3  
4 1 *Palaeogeography, Palaeoclimatology, Palaeoecology*

5  
6 2  
7  
8 3 Miocene–Pliocene rocky shores on São Nicolau (Cape Verde Islands): Contrasting  
9  
10 4 windward and leeward **biofacies** ~~biotas~~ on a volcanically active oceanic island

11  
12 5  
13  
14  
15 6 Markes E. Johnson<sup>a\*</sup>, Ricardo S. Ramalho<sup>b, c</sup>, B. Gudveig Baarli<sup>a</sup>, Mário Cachão<sup>d</sup>, Carlos  
16  
17 7 M. da Silva<sup>d</sup>, Eduardo J. Mayoral<sup>e</sup>, and Ana Santos<sup>e</sup>

18  
19  
20 8 <sup>a</sup> *Department of Geosciences, Williams College, Williamstown, MA 01267 USA*

21  
22 9 <sup>b</sup> *School of Earth Sciences, University of Bristol, Wills Memorial Building, Queens's*  
23  
24 10 *Road, Bristol, BS8 1RJ, UK*

25  
26  
27 11 <sup>c</sup> *Lamont-Doherty Earth Observatory at Columbia University, Comer Geochemistry*  
28  
29 12 *Building, P.O. Box 1000 Palisades, NY 10964 USA*

30  
31  
32 13 <sup>c</sup> *Faculdade de Ciências da Universidade de Lisboa, Departamento de Geologia e Centro*  
33  
34 14 *de Geologia, Campo Grande, 1749-016 Lisboa, Portugal*

35  
36  
37 15 <sup>d</sup> *Departamento de Geodinámica y Paleontología, Facultad de Ciencias Experimentales,*  
38  
39 16 *Universidad de Huelva, Campus de El Carmen, Avda. 3 de Marzo, s/n, 21071 Huelva,*  
40  
41 17 *Spain*

42  
43  
44 18 Corresponding author; E-mail address: [mjohnson@williams.edu](mailto:mjohnson@williams.edu)

45  
46  
47 19 Department of Geosciences, Williams College, ph (413) 597-2329; fax (413) 597-4116

48  
49 20

50  
51 21 ABSTRACT

52  
53 22 North Atlantic islands in the Cape Verde Archipelago off the coast of West Africa

54  
55 23 commonly feature an elongated N–S shape in which reduced northern coasts and longer

56  
57 24 eastern shores absorb the brunt of wave activity and long-shore currents generated by

1  
2  
3  
4  
5  
6  
7  
8  
9  
10  
11  
12  
13  
14  
15  
16  
17  
18  
19  
20  
21  
22  
23  
24  
25  
26  
27  
28  
29  
30  
31  
32  
33  
34  
35  
36  
37  
38  
39  
40  
41  
42  
43  
44  
45  
46  
47  
48  
49  
50  
51  
52  
53  
54  
55  
56  
57  
58  
59  
60  
61  
62  
63  
64  
65

25 prevailing North East Trade Winds. Located in the middle windward islands, São  
26 Nicolau is unusual in profile with an elongated E–W configuration that offers a broad  
27 target against high-energy, wind-driven waves. Conversely, the south shore of São  
28 Nicolau provides relatively wide shelter in a leeward setting. Reconstruction of the  
29 proto-island prior to the onset of the Main Eruptive stage during the Late Miocene at ~5.1  
30 Ma reveals a moderately smaller island with essentially the same E–W orientation. This  
31 study ~~summarizes~~ **combines** previous data **and new results from a detailed stratigraphic**  
32 **log based on** ~~collected from~~ Upper Miocene limestone deposits on the island’s south  
33 flank for comparison with ~~newly compiled~~ stratigraphic profiles of Upper Miocene  
34 limestone ~~with detailed stratigraphical logs~~ from the island’s northeast quarter. ~~Also~~  
35 ~~utilized are~~ **New** profiles from a Pliocene sandy limestone **outcropping** ~~exposed~~ on the  
36 south-central coast of São Nicolau **give added context to the diversity of marine**  
37 **invertebrates, including branching coral colonies and delicate ramose bryozoans that**  
38 **found shelter in a leeward setting.** Whole rhodoliths contribute the main fabric of  
39 carbonates deposited against rocky shores on the northern, exposed side of the Miocene  
40 island, whereas only traces of worn rhodoliths and rhodolith sand ~~coralline red algae~~  
41 occur **as in** finer Miocene grainstone on the island’s southern, protected side. ~~The~~  
42 ~~Pliocene~~ **succession** ~~sequence gives added context to the diversity of marine~~  
43 ~~invertebrates, including branching coral colonies and delicate ramose bryozoans that~~  
44 ~~found shelter in a leeward setting.~~ These Miocene and Pliocene carbonate deposits were  
45 terminated by submarine flows on an actively growing volcanic island. The passage zone  
46 from submarine to subaerial flows on the island’s flanks makes a useful meter-stick to  
47 gauge absolute water depth at the moment of local extinction by volcanic activity.

1  
2  
3  
4  
5  
6  
7  
8  
9  
10  
11  
12  
13  
14  
15  
16  
17  
18  
19  
20  
21  
22  
23  
24  
25  
26  
27  
28  
29  
30  
31  
32  
33  
34  
35  
36  
37  
38  
39  
40  
41  
42  
43  
44  
45  
46  
47  
48  
49  
50  
51  
52  
53  
54  
55  
56  
57  
58  
59  
60  
61  
62  
63  
64  
65

48

49 *Keywords:* Coastal deposition, Miocene, Pliocene, Rhodoliths (Rhodophyta), Northeast  
50 Trade Winds, Volcanic islands

51 **1. Introduction**

52 Islands are singular landscapes where the limits of habitability are proportionate  
53 to size and distance from the nearest mainland (MacArthur, 1972). However arrayed in  
54 the seas or oceans that surround them, islands also enforce restrictions on life subject to  
55 the wider field of prevailing winds, ocean currents, storm tracks, and other climatic  
56 factors typical for any given geographic realm. Coral species that colonized emigrated to  
57 the big island of Hawaii, for example, thrive on the leeward Kona Coast where ocean  
58 swell from the South Pacific is moderate compared to rough conditions on the windward  
59 Hamakua Coast where wave shock energized by persistent trade winds prohibits coral  
60 growth (Dollar and Tribble, 1993). On continental islands closer to a mainland,  
61 variations in physical factors between exposed, outer rocky shores and sheltered inner  
62 shores regulate the distribution of marine organisms, as found for example around the  
63 Channel Islands of southern California (Littler et al., 1991). The geological record is  
64 capable of preserving whole islands, some of which that demonstrate fossil evidence for  
65 contrasting exposed and sheltered biotopes (Johnson, 2002 Johnson and Hayes, 1993;  
66 Rong et al., 2013). Due to plate tectonics and the re-cycling of oceanic crust, the  
67 geologic record is biased in favor of continental islands leading as far back as the  
68 Cambrian (Dott, 1974). In contrast, hotspot oceanic islands are transient features due to  
69 island subsidence and strong marine erosion. Consequently, their onshore record  
70 typically does not extend beyond Miocene times (Menard, 1986). Their mid-ocean

1  
2  
3  
4  
5  
6  
7  
8  
9  
10  
11  
12  
13  
14  
15  
16  
17  
18  
19  
20  
21  
22  
23  
24  
25  
26  
27  
28  
29  
30  
31  
32  
33  
34  
35  
36  
37  
38  
39  
40  
41  
42  
43  
44  
45  
46  
47  
48  
49  
50  
51  
52  
53  
54  
55  
56  
57  
58  
59  
60  
61  
62  
63  
64  
65

71 geography, however, makes them prime localities to look at present and past coastal  
72 biotopes and sedimentary processes in an oceanic setting, as well as places to gain  
73 insights on ancient patterns of wind and ocean currents.

74 All 20 Miocene and 15 Pliocene examples of biotas associated with rocky shores  
75 from localities around the world surveyed by Johnson and Baarli (2012) come from  
76 continental shelves. Rocky-shore biotas from oceanic islands, however, are becoming  
77 better known. Santos et al. (2011) described a rocky shore from the Middle Miocene of  
78 Porto Santo in Madeira (Portugal) that features a biota with intertidal zonation.  
79 Additional studies on Miocene carbonates from Porto Santo include those by Johnson et  
80 al. (2011), Santos et al. (2012), and Baarli et al. (2013). The coastal carbonates of Porto  
81 Santo and many other oceanic islands in the northeast Atlantic Ocean often incorporate  
82 whole rhodoliths or sediments eroded from rhodoliths. These coralline red algae are non-  
83 attached and spherical to sub-spherical in shape due to concentric growth accruing with  
84 circumrotary movement in benthic settings in sun-lighted waters. Evidence collected  
85 ~~more generally~~ on a global scale suggests that rhodoliths achieved peak domination in  
86 carbonate facies ~~through and soon after the~~ during the Early to Middle Miocene times  
87 Climatic Optimum (Halfar and Mutti, 2005; Braga et al., 2010).

88 Island groups from the North Atlantic realm of Macaronesia, which include the  
89 Azores, Madeira (with the Selvagens), Canary, and Cape Verde archipelagos, have a  
90 volcanic history tracing back to the Miocene or older. Additionally, many of the  
91 Macaronesian islands were subjected to uplift, making them particularly rich in exposed  
92 marine sedimentary and volcanic sequences (Ramalho et al., 2010a, b; Ávila et al, 2012;  
93 Meireles et al., 2013). Like Madeira, the fabric of Miocene and younger limestone

1  
2  
3  
4  
5  
6  
7  
8  
9  
10  
11  
12  
13  
14  
15  
16  
17  
18  
19  
20  
21  
22  
23  
24  
25  
26  
27  
28  
29  
30  
31  
32  
33  
34  
35  
36  
37  
38  
39  
40  
41  
42  
43  
44  
45  
46  
47  
48  
49  
50  
51  
52  
53  
54  
55  
56  
57  
58  
59  
60  
61  
62  
63  
64  
65

94 deposits from many of the other island groups is enriched by rhodoliths and rhodolith-  
95 derived sediments (Mayoral et al., 2013; Johnson et al., 2012, 2013; Amen et al., 2005;  
96 Zazo et al., 2002). A theme of overarching regional interest concerns the degree to which  
97 the strong Northeast Trade Winds pervasive across **much of** Macaronesia influenced the  
98 **formation of rhodolith limestone.** ~~distribution and incorporation of rhodoliths in~~  
99 ~~limestone deposits of various kinds.~~

100 This study is focused on São Nicolau, one of the principal windward islands  
101 belonging to the Cape Verde Archipelago in southern Macaronesia off the West African  
102 coast of Senegal. **The goal of this study is to test the hypothesis that differences in past**  
103 **biofacies around the margins of the island are due to physical constraints related to**  
104 **contrasting windward and leeward environments.** Two ~~tasks~~ **goals** shape the project's  
105 organization: 1) to reconstruct the approximate size and configuration of the proto-island  
106 of São Nicolau during the Late Miocene and immediately before the onset of the Main  
107 Eruptive Complex (after Macedo et al., 1988), and 2) to compile detailed stratigraphic  
108 profiles for Miocene and Pliocene sections that include **biofacies associated with fossil**  
109 ~~biotas related to~~ former rocky shores. ~~The central hypothesis to be tested is that~~  
110 ~~differences in biotas and related bioclastics around the margins of the island are due to~~  
111 ~~physical constraints related to contrasting windward and leeward environments.~~ Presence  
112 ~~or absence of rhodoliths in the studied sections is but one factor considered among others~~  
113 ~~that entail a range of ecological dynamics regarding additional biological components.~~

114  
115 **2. Geographic and geologic settings**

116 *2.1. Physical geography*

1  
2  
3  
4  
5  
6  
7  
8  
9  
10  
11  
12  
13  
14  
15  
16  
17  
18  
19  
20  
21  
22  
23  
24  
25  
26  
27  
28  
29  
30  
31  
32  
33  
34  
35  
36  
37  
38  
39  
40  
41  
42  
43  
44  
45  
46  
47  
48  
49  
50  
51  
52  
53  
54  
55  
56  
57  
58  
59  
60  
61  
62  
63  
64  
65

117            São Nicolau is one of 15 volcanic islands in the Cape Verde Archipelago  
118 dispersed over a prominent seafloor anomaly called the Cape Verde Rise (Fig. 1). Due to  
119 an almost-stationary position with respect to its melting source, the archipelago  
120 corresponds to a cluster of islands arrayed in a west-facing crude semi-arc (McNutt,  
121 1988; Ramalho, 2011). Traditionally, the Cape Verde Islands have been classified into  
122 “windward” ~~comprising all the northernmost islands of Santo Antão, São Vicente, Santa~~  
123 ~~Luzia, São Nicolau, Sal, and Boavista~~ and “leeward” islands ~~comprising the islands of~~  
124 ~~Maio, Santiago, Fogo and Brava~~ with respect to the dominant NE trade winds. São  
125 Nicolau is one of the windward islands and it ranks fifth largest in size with an area of  
126 343 km<sup>2</sup>, which is slightly above the median compared to the 14 other Cape Verdean  
127 islands (Mitchell-Thomé, 1972, ~~his table 1~~). In terms of elevation, São Nicolau is the  
128 fourth highest with a maximum elevation of 1,304 m (Mitchell-Thomé, 1972, ~~his table 1~~).

129            The location of São Nicolau within the north-central part of the archipelago and  
130 the island’s overall shape make it an appropriate subject for this study. In particular, the  
131 north shore of São Nicolau is unusual for ~~a its~~ roughly east–west alignment that extends  
132 over a distance of 45 km (Fig. 1). No other island in the group makes such a broad target  
133 for the steady trade winds arriving out of the northeast. With little difference between  
134 winter and summer seasons, the north shore of São Nicolau is subject to winds that reach  
135 5–6 on the Beaufort Scale (Brand, 2011), which equates to wind speeds between 8 and  
136 10.8 m/sec. Intervals of calm are seldom met on this shore. Crossing an enormous fetch,  
137 the trade winds that reach São Nicolau produce ocean swells with wave heights that run  
138 between 3.5 and 6 m (Brand, 2011). The present-day wind field and sea-surface  
139 dynamics make conditions on the windward rocky shore highly energetic. Scouring of

1  
2  
3  
4  
5  
6  
7  
8  
9  
10  
11  
12  
13  
14  
15  
16  
17  
18  
19  
20  
21  
22  
23  
24  
25  
26  
27  
28  
29  
30  
31  
32  
33  
34  
35  
36  
37  
38  
39  
40  
41  
42  
43  
44  
45  
46  
47  
48  
49  
50  
51  
52  
53  
54  
55  
56  
57  
58  
59  
60  
61  
62  
63  
64  
65

140 the shore is intense and even small pocket beaches (as at the mouth of Ribeira Alta east  
141 of Juncalinho) are rare along the north coast. The island's largest ~~only substantial~~ sand  
142 beaches are found around Tarrafal de São Nicolau on the sheltered, southwest side of the  
143 island (Fig. 1).

144  
145 *2.2. History of volcanism*

146 São Nicolau corresponds to an elongated shield volcano in an early post-erosional  
147 stage of development. The island's geomorphology and structure indicate development  
148 by composite fissure volcanism along two main rift arms. The more prominent is  
149 oriented E–W to WNW–ESE in direction, whereas the lesser is oriented N–S comprising  
150 the western portion of the island (Ramalho et al., 2010a). The island's volcanic history  
151 extends from the Miocene to the Quaternary (Macedo et al., 1988; Duprat et al., 2007;  
152 Ramalho et al., 2010a, b).

153 Emergence of the earliest landmass belonging to present-day São Nicolau  
154 occurred sometime during the Mid- to Late Miocene and corresponds to the Old Eruptive  
155 Complex. This unit, which remains undated, mostly comprises intensely palagonitized  
156 hyaloclastites pervasively intruded by a dyke swarm (Macedo et al., 1988; Ramalho,  
157 2011). Marine sediments and submarine lavas rest unconformably above this unit. The  
158 first corresponds to shallow-water calcarenites (Monte Focinho Formation) with an  
159 ~~estimated age interpreted~~ between 11.8 and 5.8 Ma or even between 6.2 and 5.8 Ma  
160 (Bernoulli et al., 2007), whereas the latter corresponds to an entirely submarine volcanic  
161 unit (Figueira de Coxe Formation) that erupted between 6.2 and 5.8 Ma (Duprat et al.,  
162 2007; Ramalho et al., 2010b). The Figueira de Coxe Formation crops out at elevations in

1  
2  
3  
4 163 excess of 270 m above sea level attesting to episodic uplift that has affected São Nicolau  
5  
6 164 since its first emergence above sea level (Ramalho et al., 2010a, b, c).

7  
8  
9 165 After a brief period of volcanic quiescence, uplift, and erosion, during which  
10  
11 166 coastlines and adjacent shelves matured, the edifice of São Nicolau experienced a period  
12  
13 167 of renewed and vigorous volcanic activity that corresponds to the Main Eruptive  
14  
15 168 Complex (Macedo et al., 1988; Ramalho et al. 2010a, b). During this stage, coastlines  
16  
17 169 rapidly expanded considerably (and rapidly) by lateral progradation of effusive lava  
18  
19 170 deltas that covered large swaths of the pre-existing island shelf and preserved existing  
20  
21 171 shelf sediments within the volcanic sequence. The main shield-building stage on São  
22  
23 172 Nicolau lasted approximately 2.5 million years, from 5.0 to 2.5 Ma before present  
24  
25 173 (Duprat et al., 2007; Ramalho et al., 2010b), a period during which coastlines constantly  
26  
27 174 and rapidly shifted as volcanic activity and erosion counterbalanced each other. Finally,  
28  
29 175 around 2.5 Ma, São Nicolau entered a period of slow erosional decay, interrupted by two  
30  
31 176 intervals of volcanic rejuvenation that correspond to the Preguiça and Monte Gordo  
32  
33 177 formations, respectively at 1.7–0.7 Ma and <100 ka (Duprat et al., 2007; Ramalho et al.,  
34  
35 178 2010b).

36  
37  
38  
39  
40  
41  
42  
43 179

### 44 180 *2.3. Previous paleontological studies*

45  
46 181 Earlier studies on the paleontology of São Nicolau were conducted by Bebiano  
47  
48 182 (1932), Torres and Soares (1946), Serralheiro and Ubaldo (1979), and Macedo et al.  
49  
50 183 (1988). Torres and Soares (1946) identified some species of fossil rhodoliths belonging  
51  
52 184 to the genus *Lithothamnion*, including material from Monte Focinho. A more recent  
53  
54 185 study by Bernoulli et al. (2007) provided a reappraisal of the taxonomy and age of key  
55  
56  
57  
58  
59  
60  
61  
62  
63  
64  
65



1  
2  
3  
4 186 fossils from the limestone at Monte Focinho near the island's south-central coast (Fig. 1).  
5  
6 187 A Late Miocene age was established both on the basis of benthic foraminifera in the  
7  
8 188 genus *Amphistegina* and planktic foraminifera attributed assigned to various species of  
9  
10 189 *Globigerina*, *Globigerinoides*, *Globorotalia*, and other genera. The grainstone from this  
11  
12 190 locality includes the abundant debris of cirripede barnacles mixed with lesser amounts  
13  
14 191 of coralline red algae fragments that accumulated below a steep, rocky shore.

15  
16 192 Previously shown in part by Macedo et al., (1988), recent mapping by Ramalho et  
17  
18 193 al. (2010a) traced a distinct band of Miocene limestone along São Nicolau's southeastern  
19  
20 194 coast to Ponta Barroso (Fig. 1). Sea cliffs along this stretch of the coast are sheer and  
21  
22 195 difficult to access without the use of specialized climbing equipment. However, the  
23  
24 196 exposure near the tip of Ponta Barroso is accessible by an arduous overland route. Field  
25  
26 197 notes and field photos collected by one of us (RSR) at Ponta Barroso record the  
27  
28 198 occurrence of fine grainstone calcarenite with rare large echinoids and bivalves, as well  
29  
30 199 as small pectens. Some rhodolith debris is restricted to the base of the unit. No whole  
31  
32 200 rhodoliths were observed. The thickness of this unit is about 1 m, but varies up to a  
33  
34 201 maximum of about 3 m in thickness.

35  
36  
37  
38  
39  
40  
41  
42  
43 202

### 44 203 **3. Methods**

45  
46 204 The approximate size and configuration of the island of São Nicolau during the  
47  
48 205 Late Miocene and immediately prior to the onset of the Main Eruptive stage at ~5.1 Ma  
49  
50 206 (Ramalho et al., 2010b) was reconstructed using the present outcrop pattern of the Old  
51  
52 207 Eruptive Complex and Figueira de Coxe Formation in conjunction with relative sea-level  
53  
54 208 information extracted from the volcanic succession sequence at Castilhano (sometimes  
55  
56  
57  
58  
59  
60  
61  
62  
63  
64  
65

1  
2  
3  
4  
5  
6  
7  
8  
9  
10  
11  
12  
13  
14  
15  
16  
17  
18  
19  
20  
21  
22  
23  
24  
25  
26  
27  
28  
29  
30  
31  
32  
33  
34  
35  
36  
37  
38  
39  
40  
41  
42  
43  
44  
45  
46  
47  
48  
49  
50  
51  
52  
53  
54  
55  
56  
57  
58  
59  
60  
61  
62  
63  
64  
65

209 written Castilhiano). In this place, the first erupted lavas of the Main Eruptive Complex  
210 (dated at 5.09±0.07 Ma) preserved a paleo-coastline that presently can be found at ~100  
211 m of elevation (Ramalho et al., 2010a,b). Thus, using ~~the sequence at the~~ Castilhano  
212 **succession** as a pivot point, the shape and dimensions of proto-São Nicolau were  
213 extrapolated around the perimeter defined by all outcrops of the Old Eruptive Complex  
214 and Figueira de Coxe Formation **pene-contemporaneous in position** ~~that can be found~~  
215 ~~above ~100 m above present-day sea level~~. On the northern coast, where marine erosion  
216 already reduced the island considerably, the approximate position of the 100-m isobath  
217 was used to speculate where the northern limit of the ~~Late Miocene~~ island edifice was  
218 located **during the Late Miocene**.

219           Strip logs for stratigraphic sections modified after the standard format used by  
220 Shell Oil Company were compiled for four localities divided between the north and south  
221 shores of São Nicolau. In addition to rhodoliths, care was taken to register occurrences  
222 of shelly macrofossils and trace fossils. Samples also were collected for calcareous  
223 nannofossils, generally limited to finer grained and less indurated layers in the carbonate  
224 succession. The fine fractions from samples were concentrated in laboratory test tubes  
225 through overnight settling from a vigorously shaken half-sediment, half-tap-water  
226 suspension. The top fine fraction was extracted directly to a cover glass by a Pasteur  
227 pipette, spread into a rippled smear, and permanently mounted. Smear slides were  
228 scanned for coccoliths on a petrographic microscope (Zeiss Ortholux II-Pol) at x1250  
229 magnification along a 3-cm column (approximately 5 mm<sup>2</sup>). Calcareous nannofossil  
230 taxonomy follows criteria standardized by Perch-Nielsen (1985) and Bown (1998).

1  
2  
3  
4  
5  
6  
7  
8  
9  
10  
11  
12  
13  
14  
15  
16  
17  
18  
19  
20  
21  
22  
23  
24  
25  
26  
27  
28  
29  
30  
31  
32  
33  
34  
35  
36  
37  
38  
39  
40  
41  
42  
43  
44  
45  
46  
47  
48  
49  
50  
51  
52  
53  
54  
55  
56  
57  
58  
59  
60  
61  
62  
63  
64  
65

231 Rhodolith samples from two levels at Castilhano were collected for identification at the  
232 genus level using petrographic thin sections.

233 Whole rhodolith specimens from specific stratigraphic intervals were measured  
234 on site (to the nearest millimeter) across three principal axes (long, intermediate, and  
235 short). Data from these measurements were subjected to analysis based on the triangular  
236 plot among spherical, ellipsoidal, and discoidal shapes according to the format applied to  
237 rhodoliths by Bosence (1976, 1983) as modified from Sneed and Folk (1958).

238

239 **4. Results**

240 *4.1. Island reconstruction for the ~~of a~~ Late Miocene island*

241 Coastline reconstructions for a Late Miocene (5.7–5.1 Ma) island indicate an  
242 elongated edifice approximately 25–33 km in length in an east-west dimension, and at  
243 least 8-10 km of maximum width in the north-south dimension (Fig. 2). The lack of  
244 outcrops of the Old Eruptive Complex and Figueira de Coxe Formation in an area east of  
245 Juncalinho and in the vicinities of Ribeira Alta precludes any more solid reconstructions  
246 for this part of the edifice.

247

248 *4.2. North shore stratigraphy and paleontology*

249 Stratigraphic profiles from the oasis at Castilhano and the canyon walls of Ribeira  
250 de Covoada de Bodela (Fig. 3) detail the onlap of carbonate deposits against rocky shores  
251 located on the northeast flank of Miocene São Nicolau (Figs. 1–2). Both sections are  
252 constrained below by the Old Eruptive Complex (intensely altered hyaloclastites and  
253 basaltic lava flows) and above by basaltic lava flows belonging to the onset of the Main

1  
2  
3  
4  
5  
6  
7  
8  
9  
10  
11  
12  
13  
14  
15  
16  
17  
18  
19  
20  
21  
22  
23  
24  
25  
26  
27  
28  
29  
30  
31  
32  
33  
34  
35  
36  
37  
38  
39  
40  
41  
42  
43  
44  
45  
46  
47  
48  
49  
50  
51  
52  
53  
54  
55  
56  
57  
58  
59  
60  
61  
62  
63  
64  
65

254 Eruptive Complex. Both sections include abundant rhodoliths and both replicate a  
255 fining-up pattern through the first 3-4 m at which point the Bodela section terminates.  
256 Thereafter, the Castilhano section recommences with renewed coarsening and rhythmic  
257 fining and coarsening in thick beds before a final fining-upwards sequence. The lower  
258 part of the carbonate succession at Castilhano is packed with rhodoliths that over-ride an  
259 irregular basalt surface with a topographic relief of about 1 m, including small overhangs  
260 of basalt under which rhodoliths are trapped (Fig. 4A and B). ~~In places, the original~~  
261 ~~basalt surface features thin algal patches attributed to coralline red algae.~~ A basalt  
262 boulder above the unconformity exhibits a cluster of circular depressions 4 cm in  
263 diameter (Fig. 4C) that match the typical dwelling structures of regular echinoids  
264 assigned to the ichnospecies *Circolites kotoncensis*. Rhodoliths are less common in the  
265 stratigraphic interval between 2.5 m to 4 m above the unconformity, but thereafter  
266 resume in abundance (Fig. 3). An interval directly below the 4-m horizon features the  
267 trace fossil *Thalassinoides suevicus* (Fig. 4D).

268 Many rhodoliths reveal a small rock core of basalt in cross section (Fig. 4E).  
269 Sampled from a horizon 40 cm above the unconformity, the average maximum diameter  
270 of rhodoliths is 3.3 cm. Higher at a level 2.5 m above the unconformity, the average  
271 maximum diameter of rhodoliths registers an increase to 3.75 cm. **The rhodoliths from**  
272 **these two levels are identified as belonging to the genus *Lithothamnion* (Davide Bassi,**  
273 **personal communication, 2013).** Pectinid bivalves and *Spondylus* sp. together with  
274 broken tests of the echinoid *Clypeaster* sp. are more common in the upper half of the  
275 exposure than in the lower half. Loose plates of the cirriped barnacle *Balanus* sp. appear  
276 in the top two meters of the exposure.

1  
2  
3  
4  
5  
6  
7  
8  
9  
10  
11  
12  
13  
14  
15  
16  
17  
18  
19  
20  
21  
22  
23  
24  
25  
26  
27  
28  
29  
30  
31  
32  
33  
34  
35  
36  
37  
38  
39  
40  
41  
42  
43  
44  
45  
46  
47  
48  
49  
50  
51  
52  
53  
54  
55  
56  
57  
58  
59  
60  
61  
62  
63  
64  
65

277           At half the thickness of the Castilhana section, the Bodela section (Fig. 3) also  
278 exhibits an unconformity surface with about 1 m of relief on submarine basalt but is  
279 notably different in development of a distinct basal conglomerate with eroded clasts up to  
280 45 cm in diameter (Fig. 4F). Rhodoliths with an average maximum diameter of 3.5 cm  
281 are plentiful through the overlying section, but not quite as abundant as found in the  
282 Castilhana section. In addition to *Pecten* sp. and *Spondylus* sp., ~~additional~~ **associated**  
283 bivalves include oysters encrusted on basalt boulders and the infaunal bivalves *Cardium*  
284 sp. and *Venus* sp. As at Castilhana, broken pieces of tests belonging to *Clypeaster* sp.  
285 occur, but also the spines of a cidaroid echinoid. Barnacles appear in the Bodela section  
286 attached only to bivalves. ~~Broken~~ **Rare** pieces of the finger coral *Porites* sp. represent a  
287 faunal element at Bodela not observed at Castilhana.

288

289 *4.3. Fossil rhodolith shape analyses*

290           Although the shallow-water marine **assemblages** ~~faunas~~ of Castilhana and Bodela  
291 are somewhat diverse, rhodoliths are the dominant element contributing to the limestone.  
292 Samples of whole rhodoliths varying in number from 35–40 specimens were extricated  
293 for measurements from narrowly defined stratigraphic intervals at both localities.  
294 **Comparison shows that** the most spheroidal rhodoliths come from an interval 40 cm  
295 above the base of the Castilhana section with a spread almost entirely restricted to the  
296 upper triangle in the larger triangular plot (Fig. 5A). Higher in the Castilhana section  
297 (2.5 m above the unconformity), rhodoliths are slightly larger in size and **exhibit** a slight  
298 tendency to more ellipsoidal shapes indicated by the spill-over of roughly half the sample  
299 into other sectors below and to the right of the upper triangle (Fig. 5B). The rhodolith

1  
2  
3  
4  
5  
6  
7  
8  
9  
10  
11  
12  
13  
14  
15  
16  
17  
18  
19  
20  
21  
22  
23  
24  
25  
26  
27  
28  
29  
30  
31  
32  
33  
34  
35  
36  
37  
38  
39  
40  
41  
42  
43  
44  
45  
46  
47  
48  
49  
50  
51  
52  
53  
54  
55  
56  
57  
58  
59  
60  
61  
62  
63  
64  
65

300 sample from the Bodela section (Fig. 5C) comes from a level directly above the basal  
301 conglomerate (Fig. 3). In the range of shapes, it is more like the lower sample from  
302 Castilhano, but with a very few points that spill outside the upper triangle in a pattern  
303 similar to the upper sample from Castilhano. The majority of rhodoliths from both  
304 sections is highly uniform in **size and** shape.  ~~, showing forms that are easily rolled by the~~  
305 ~~movement of the water mass related to surface waves or bottom currents.~~

306  
307 *4.4. South shore stratigraphy and paleontology*

308 **A stratigraphic profile from Baía dos Barreiros (Fig. 6) details the onlap of carbonate**  
309 **deposits against rocky shores eroded in the Old Eruptive Complex located on the**  
310 **southeast flank of Miocene São Nicolau (Fig. 2). In this region, the carbonates crop out**  
311 **near the base of sea cliffs for 2.5 km from Baía dos Barreiros to Ponta Barroso (Fig. 2).**  
312 **Sediments constitute a 4 to 5 m evenly thick band, dipping about 10° to the south. In**  
313 **detail, however, the internal structure exhibits prograding foresets dipping about 15–20°**  
314 **to the south. Sediment composition is overwhelmingly dominated by intermediate-to-**  
315 **coarse rhodolith debris with very low amounts of lithics. Abraded rhodoliths are present**  
316 **but extremely rare, as well as other macrofossils. The succession generally exhibits a**  
317 **fining-up pattern, but terminates with a conglomerate that features pebbles derived from**  
318 **the Old Eruptive Complex (Fig. 6). Intervals with the trace-fossil *Thalassinoides* isp.**  
319 **occur at 1.25 m and 3.8 m above the base of the section; the trace-fossils *Sinusichnus* isp.**  
320 **and *?Ophiomorpha* isp appear at a horizon 3 m above the base of the section. These**  
321 **trace-fossils are known to have a wide depth range in littoral to outer shoreface settings**  
322 **(Mayoral et al., 2013). An erosive unconformity is inferred at the top of the sedimentary**

1  
2  
3  
4  
5  
6  
7  
8  
9  
10  
11  
12  
13  
14  
15  
16  
17  
18  
19  
20  
21  
22  
23  
24  
25  
26  
27  
28  
29  
30  
31  
32  
33  
34  
35  
36  
37  
38  
39  
40  
41  
42  
43  
44  
45  
46  
47  
48  
49  
50  
51  
52  
53  
54  
55  
56  
57  
58  
59  
60  
61  
62  
63  
64  
65

323 succession, as shown by truncation of a basaltic dyke. The sediments along Baía dos  
324 Barreiros occur at the same stratigraphic position found at Castilhano and Ribeira de  
325 Covoada de Bodela. As such, these sections are considered to be pene-contemporaneous.

326 Extensive sedimentary outcrops on the south shore are exposed through the  
327 canyon of the Ribeira da Ponta da Pataca, located about 800 m south-southwest of the  
328 village of Preguiça (Fig. 1). Stratigraphic profiles for Pataca 1 (Fig. 6) and Pataca 2 (Fig.  
329 7) are laterally continuous over 130 m and represent respective distal and more proximal  
330 settings in relationship to a former paleoshore. The thicker succession sequence at Pataca  
331 1 commences 17 m above present sea level, whereas the thinner succession sequence at  
332 Pataca 2 starts at about 60 m above present sea level and follows inland along the narrow  
333 streambed of Ribeira da Ponta da Pataca. Well-defined beds near the top of the  
334 succession dip about 6 to 8° to the southeast. A pile of submarine sheet flows rest  
335 conformably above the fossiliferous sediments. The transition to subaerial flows is  
336 poorly observed as the outcrops are extensively covered by scree.

337 At Pataca 1, the outcrop consists of three coarsening-up intervals with echinoid  
338 tests and spines present throughout. The initial coarsening-up sequence is a massive,  
339 very sandy and poorly sorted limestone or calcareous sandstone (Fig. 8A). Whole  
340 macrofossils are few, but the bivalve *Pinna* sp. is preserved in life position. In addition,  
341 short branching colonies of *Porities* sp. (Fig. 8B) occur together with thin, stick-shaped  
342 bryozoans of *Thalamoporella* sp. (Fig. 8C) that are commonly encrusted by a more  
343 delicate bryozoan attributed to *Metrarabdotos* sp. The trace fossils *Ophiomorpha nodosa*  
344 and *Macaronichnus segregatis* range through most of the initial interval. A second  
345 coarsening-up interval is a more pure limestone with higher fossil content that includes

1  
2  
3  
4  
5  
6  
7  
8  
9  
10  
11  
12  
13  
14  
15  
16  
17  
18  
19  
20  
21  
22  
23  
24  
25  
26  
27  
28  
29  
30  
31  
32  
33  
34  
35  
36  
37  
38  
39  
40  
41  
42  
43  
44  
45  
46  
47  
48  
49  
50  
51  
52  
53  
54  
55  
56  
57  
58  
59  
60  
61  
62  
63  
64  
65

346 coral fragments and coquinas of *Argopecten* aff. *flabellum* (Fig. 8D). *Balanus* plates also  
347 are present. Many fossils are encrusted by bryozoans and serpulids. The trace fossil  
348 *Ophiomorpha nodosa* occurs at the very base of the interval, but otherwise trace fossils  
349 are absent. A third coarsening-up interval begins with minor basalt clasts and changes to  
350 a well-sorted lithic sandstone with little fossil content. Echinoids are the most common  
351 fossils in this interval, but *Balanus* plates also are present. The trace fossil *Skolithos*  
352 *linearis* (Fig. 8E) dominates the top 60 cm of this interval. The sediments seem to rest  
353 upon volcanoclastic breccia that may correspond to collapsed material and/or deposits of  
354 submarine debris flows.

355       The upper part of Pataca 1 is physically continuous with the lower part of Pataca  
356 2. Being more proximal, however, Pataca 2 differs laterally in exhibiting a much higher  
357 content of basaltic clasts (Fig. 8F). The section shows a change from sandy limestone to  
358 calcareous sandstone (Fig. 7) with increasingly better sorting. The trace fossil  
359 *Thalassinoides suevicus* occurs near the base of the section. The lower layers are very  
360 fossiliferous, changing upwards to more **bioclastic content** ~~broken shells~~. The  
361 gastropods *Strombus* sp. and *Turritella* sp. together with pectinid bivalves and barnacles  
362 are very common. Some coral colonies of *Tubastrea* sp. with conspicuous borings by  
363 pholad bivalves (Fig. 8G) are encrusted together with serpulids on basalt cobbles. The  
364 upper part of this section is formed by massive sandstone with fewer fossils. Echinoids  
365 spines, transported and worn *Porites* colonies and **fragments of** ~~broken~~ *Pecten* shells are  
366 present, as well as a sparse representation of the trace fossil *Ophiomorpha nodosa*.

367  
368 4.5. *Calcareous nannofossil biostratigraphy*



1  
2  
3  
4  
5  
6  
7  
8  
9  
10  
11  
12  
13  
14  
15  
16  
17  
18  
19  
20  
21  
22  
23  
24  
25  
26  
27  
28  
29  
30  
31  
32  
33  
34  
35  
36  
37  
38  
39  
40  
41  
42  
43  
44  
45  
46  
47  
48  
49  
50  
51  
52  
53  
54  
55  
56  
57  
58  
59  
60  
61  
62  
63  
64  
65

369 Samples for age-diagnostic nanofossils were collected at three levels through the  
370 stratigraphic succession at Castilhano (see Fig. 3) both with and without rhodoliths.  
371 Species common to all three samples include *Dictyococcites antarticus*, *D. productus*,  
372 *Reticulofenestra haqii-minutula*, and *R. pseudoumbilicus*. The abundance of calcareous  
373 nanofossils showed an increase up-section, consistent with the transgressive nature of  
374 the succession. No species were exclusive to the horizon rich in rhodoliths. Species  
375 common to the upper samples but lacking from the lowest sample include *Calcidiscus*  
376 *leptoporus*, *Ciclicargolithus floridanus*, *Discaster* sp., small *Reticulofenestra* sp., *R.*  
377 *rotaria*, *Sphenolithus abies*, and *Syracosphaera* sp. The assemblage is compatible with a  
378 **Late Miocene** ~~an Upper Miocene position, in particular the~~ (Messinian) age (Bown,  
379 1998). Notably, *R. rotaria* has a know First Appearance Datum (FAD) of 7.42 Ma and  
380 Last Appearance Datum (LAD) of 6.91 Ma.

381 A single sample was collected from the up-stream section at Ribeira Covoada de  
382 Bodela (see Fig. 3). The diversity of calcareous nanofossils is lower than **that** found at  
383 any level at Castilhano, but includes many of the same species indicative of correlation  
384 with the Messinian Stage.

385 Samples were collected at three levels through the Pataca 1 section (see Fig. 7).  
386 The sample from the lower layers is low in diversity with only three species:  
387 *Braarudosphaera* cf. *rosa*, *Coronocylus nitescens*, and *Discoaster* sp. The sample from  
388 the middle layers proved to be barren of nanofossils. Finally, a sample from the upper  
389 layers yielded an assemblage including *Calcidiscus leptoporus*, *Coccolithus pelagicus*,  
390 *Helicosphaera carteri*, *Reticulofenestra productus*, *R. minuta*, *R. haquii-minutula*, *R.*  
391 *antarticus*, *R. pseudoumbilicus*, *Pontosphaera* sp. and *Umbilicosphaera* sp. This

1  
2  
3  
4  
5  
6  
7  
8  
9  
10  
11  
12  
13  
14  
15  
16  
17  
18  
19  
20  
21  
22  
23  
24  
25  
26  
27  
28  
29  
30  
31  
32  
33  
34  
35  
36  
37  
38  
39  
40  
41  
42  
43  
44  
45  
46  
47  
48  
49  
50  
51  
52  
53  
54  
55  
56  
57  
58  
59  
60  
61  
62  
63  
64  
65

392 assemblage is compatible with a Pliocene position due to the presence of several  
393 reticulofenestrids, including *R. pseudoumbilicus* (Bown, 1998).

394

395 *4.6. Summary of dichotomous biofacies*

396 ~~Using paleontological data collected by Bernoulli et al. (2007) on an Upper~~  
397 ~~Miocene deposit at Monte Focinho near the south-central coast of São Nicolau (Fig. 1), it~~  
398 ~~is instructive to draw contrasts with Upper Miocene deposits at Castilhano and Bodela~~  
399 ~~(Fig. 3) near the island's present-day northeastern shore. Using biofacies from the~~  
400 ~~northerly Upper Miocene deposits at Castilhano and Bodela (Fig. 3), it is instructive to~~  
401 ~~draw contrasts with the southerly pene-contemporaneous deposits from Baía dos~~  
402 ~~Barreiros (Fig. 6), augmented by data collected by Bernoulli et al. (2007) from the south-~~  
403 ~~central coast of São Nicolau. All four successions three are seated on the Old Eruptive~~  
404 ~~Complex as defined by Macedo et al. (1988). These deposits also signify the marine~~  
405 ~~onlap of rocky shores that are Late Miocene in age. Loose barnacle plates are present at~~  
406 ~~the Monte Focinho and Castilhano localities, as well as whole barnacles attached to shells~~  
407 ~~at Bodela, indicating an initially a relatively shallow-water source for the deposits.~~  
408 Likewise, dwelling structures eroded by regular echinoids in a basalt boulder at  
409 Castilhano (Fig. 4C) confirm such a relationship. In addition to the various benthic and  
410 planktic foraminifera recovered from the Monte Focinho section, Bernoulli et al. (2007)  
411 described a bioclastic grainstone that incorporates echinoid spines and bits of red algae,  
412 although the limestone's dominant signature comes from barnacle debris. No traces of  
413 whole or fragmentary rhodoliths were detected during our visit to the Monte Focinho  
414 locality.

1  
2  
3  
4  
5  
6  
7  
8  
9  
10  
11  
12  
13  
14  
15  
16  
17  
18  
19  
20  
21  
22  
23  
24  
25  
26  
27  
28  
29  
30  
31  
32  
33  
34  
35  
36  
37  
38  
39  
40  
41  
42  
43  
44  
45  
46  
47  
48  
49  
50  
51  
52  
53  
54  
55  
56  
57  
58  
59  
60  
61  
62  
63  
64  
65

415 Further comparisons may be drawn between the Miocene sequence at Castilhano  
416 and the Pliocene sequence at Pataca. The former registers two deepening phases of  
417 deposition on an open marine sublittoral platform signified by rhythmic fining-upward  
418 beds in the middle of the **succession** sequence (Fig. 3). In contrast, the Pataca 1 section  
419 records three coarsening-upward phases with considerably greater content of terrestrial  
420 lithics (Fig. 6). Of these, only the two upper sequences shallow sufficiently to reach  
421 relatively high-energy conditions. The presence of both whole and crushed valves  
422 belonging to pectinid bivalves indicates landward transport from an open, offshore area  
423 to the south, whereas barnacles record input from a closer, near-shore zone. This overall  
424 scenario has implications for the development of a distal delta on the leeward side of São  
425 Nicolau. The most striking omission from this Pliocene scenario is the complete lack of  
426 rhodoliths or rhodolith debris ~~brought landward from offshore areas~~. This is in marked  
427 contrast to the older Castilhano and Bodela sections on the windward side of São  
428 Nicolau, where ~~coralline red algae encrusted around basalt pebbles~~ as rhodoliths (Fig. 4F)  
429 constitute the primary carbonate signature showing shoreward transport against rocky  
430 shores. For the most part, these deposits signify death assemblages, because  
431 photosynthesis by the coralline red algae ceased for all but the top layer of rhodoliths in  
432 the transported package.

434 **5. Discussion**

435 *5.1. Reconfiguration of a Miocene island*

436 The coastline reconstructions for a Late Miocene island (Fig. 2) portray a smaller  
437 edifice than the present-day São Nicolau. This is not surprising, as these reconstructions

1  
2  
3  
4  
5  
6  
7  
8  
9  
10  
11  
12  
13  
14  
15  
16  
17  
18  
19  
20  
21  
22  
23  
24  
25  
26  
27  
28  
29  
30  
31  
32  
33  
34  
35  
36  
37  
38  
39  
40  
41  
42  
43  
44  
45  
46  
47  
48  
49  
50  
51  
52  
53  
54  
55  
56  
57  
58  
59  
60  
61  
62  
63  
64  
65

438 correspond to a moment in time that immediately preceded the onset of the main shield  
439 building stage, during which the island grew considerably in size. Notwithstanding its  
440 ~~this smaller size and the uncertainties associated with such extrapolations, it is possible to~~  
441 ~~infer that~~ São Nicolau already constituted a prominent east-west elongated volcanic  
442 edifice that extended from 25 to 33 km in length during the Late Miocene. This volcanic  
443 edifice essentially emerged above the sea surface by means of uplift and not summit  
444 volcanism, as attested to by onlap of a dominantly subaerial Main Eruptive Complex over  
445 the eroded remains of an entirely submarine edifice corresponding to the Old Eruptive  
446 Complex and Figueira de Coxe Formation.

448 *5.2. Composition and morphodynamics of São Nicolau rhodoliths*

449 The Upper Miocene rhodoliths from the northern shores of São Nicolau are  
450 characterized by three key traits. They are comparatively small, exceedingly well  
451 rounded, and are represented by the single genus *Lithothamnion*. As demonstrated  
452 through shape analyses (Fig. 5), these rhodoliths are among the most spherical detected  
453 so far in studies on living and fossil rhodoliths from the Cape Verde and Canary islands  
454 (Johnson et al., 2012). Practically, such shapes make good rollers that are susceptible to  
455 transport; therefore it is not surprising to find thick rhodolith accumulations on the  
456 windward side of paleoislands. According to Braga et al. (2010), the taxonomic  
457 composition of Miocene coralline assemblages and growth forms changes with depth that  
458 parallels present-day conditions. For example, the mastophoroid and lithophylloid  
459 rhodoliths are typical of shallower-water settings, whereas the melobesioids (which  
460 include *Lithothamnion*) tend to represent deeper-water settings. On this basis, it may be

1  
2  
3  
4  
5  
6  
7  
8  
9  
10  
11  
12  
13  
14  
15  
16  
17  
18  
19  
20  
21  
22  
23  
24  
25  
26  
27  
28  
29  
30  
31  
32  
33  
34  
35  
36  
37  
38  
39  
40  
41  
42  
43  
44  
45  
46  
47  
48  
49  
50  
51  
52  
53  
54  
55  
56  
57  
58  
59  
60  
61  
62  
63  
64  
65

461 argued that the São Nicolau rhodoliths that typically nucleate around small basalt cores  
462 were transported shoreward from deeper waters.

463           The sedimentological signature imparted by rhodoliths on the paleoshores of  
464 Miocene São Nicolau are strongly related to physical transportation. On the northeast  
465 shore at Castilhano and Bodela (Fig. 3), relatively small rhodoliths were left intact but  
466 rolled shoreward by the action of strong surf to abut directly against rocky shores. In  
467 some cases, the rhodoliths fill spaces below bedrock overhangs. In contrast, the fact that  
468 only rhodolith debris is present on the leeward southern shores at Ponta Barroso and Baía  
469 dos Barreiros (Figs. 2 and 6) indicates that long-shore currents and wave refraction was  
470 the dominant influence in transporting materials to the southern shelf. The internal  
471 structure of these beds with distinct foresets suggests that sediments were deposited as  
472 clinoforms directed offshore to the south.

473  
474 *5.3. Comparison with other windward-leeward systems*

475 ~~———Cambrian biotopes around former continental islands provide little or no evidence~~  
476 ~~regarding the imposition of windward-leeward systems, but sedimentological~~  
477 ~~relationships give some insight. Studying Precambrian-Cambrian unconformities~~  
478 ~~exposed in the Baraboo district of Wisconsin, Dott (1974) reconstructed a windward-~~  
479 ~~leeward system impacted by trade winds and storm winds that preferentially left a down-~~  
480 ~~current trail of smaller quartzite pebbles on one flank of an archipelago while leaving~~  
481 ~~much larger quartzite boulders in place around the island shores.~~

482 ~~———Sedimentological and palaeontological data collected by Rong et al. (2013) are~~  
483 ~~related to the reconstruction of a Late Silurian continental island affected by prevailing~~

1  
2  
3  
4  
5  
6  
7  
8  
9  
10  
11  
12  
13  
14  
15  
16  
17  
18  
19  
20  
21  
22  
23  
24  
25  
26  
27  
28  
29  
30  
31  
32  
33  
34  
35  
36  
37  
38  
39  
40  
41  
42  
43  
44  
45  
46  
47  
48  
49  
50  
51  
52  
53  
54  
55  
56  
57  
58  
59  
60  
61  
62  
63  
64  
65

~~484 trade winds over the flooded Sino-Korean tectonic plate. Strata sitting on diorite around  
485 the palaeoisland's circumference feature coarse, diorite-derived conglomerate on the  
486 exposed, windward flank and silty limestone in direct contact with the unconformity  
487 surface on the opposite flank. Large stromatoporids are cemented on the unconformity  
488 surface and a fauna consisting of heliolitoid and tabulate corals occurs at or very close to  
489 the unconformity surface on the protected side of the island. None of the corals occur on  
490 the windward side where the conglomerate is well developed (Rong et al., 2013).  
491 ——— A windward leeward system of opposing facies around small continental islands  
492 of Late Cretaceous age on the Pacific coast of Mexico's Baja California were described  
493 by Johnson and Hayes (1993). In this case, small rhodoliths with pebble-size cores of  
494 andesite eroded from the developing unconformity surface are embanked on the exposed  
495 flank of a paleoisland. Valves of a rudistid bivalve also are attached directly to the  
496 andesite surface on the same side of the island. These elements are absent from the  
497 opposite, leeward side of the palaeoisland, where instead oysters and bryozoans are  
498 encrusted on the unconformity and related andesite clasts in addition to cidaroid  
499 echinoids intact within the spaces among boulders.~~

500           Examples cited above originate from the literature (e.g. Johnson, 2002; Johnson  
501 and Baarli, 2012) typically relate to former islands on flooded continental shelves. The  
502 only case of a windward and leeward system previously studied from a fully oceanic  
503 setting on a basalt island comes from Porto Santo in the Madeira archipelago. At the  
504 Cabeço das Laranjas on the windward one side of Ilhéu de Cima off Porto Santo, thick  
505 Middle Miocene deposits of large rhodoliths represented by the genera Lithothamnion,  
506 Sporolithon, and Neogoniolithon are impounded against the original basalt shore

1  
2  
3  
4  
5  
6  
7  
8  
9  
10  
11  
12  
13  
14  
15  
16  
17  
18  
19  
20  
21  
22  
23  
24  
25  
26  
27  
28  
29  
30  
31  
32  
33  
34  
35  
36  
37  
38  
39  
40  
41  
42  
43  
44  
45  
46  
47  
48  
49  
50  
51  
52  
53  
54  
55  
56  
57  
58  
59  
60  
61  
62  
63  
64  
65

507 (Johnson et al., 2011). As in the Castilhano and Bodela sections on São Nicolau,  
508 rhodoliths in such transported deposits were deprived of sunlight and soon perished. ~~Life~~  
509 ~~continued at the Cabeço das Laranjas in the sense that some rhodoliths at the top of the~~  
510 ~~heap became the substrate for encrusting corals (Johnson et al., 2011, their fig. 4D).~~ In  
511 contrast, the opposite **leeward** rocky shore of Ilhéu de Cima at Pedra de Água features a  
512 coeval Middle Miocene setting with coral colonies fixed in growth position on basalt  
513 mounds that rise above a sandy zone over which no more than one or two layers of  
514 rhodoliths are emplaced (Santos et al., 2012, their figs. 1 and 9). Nearly all the rhodoliths  
515 observed in cross-section at Pedra de Água are nucleated around large basalt pebbles,  
516 whereas many of the rhodoliths at the Cabeço das Laranjas lack a rock core. The  
517 rhodoliths at Pedra de Água are **polyspecific from the genera *Lithophyllum* and**  
518 ***Sporolithon* and** considered to have grown in shallow, subtidal waters close to the  
519 paleoshore (Santos et al., 2012), whereas those at the Cabeço das Laranjas were swept  
520 towards land from deeper waters by major storms of hurricane strength (Johnson et al.,  
521 2011).

523 *5.3. Shifting Miocene wind and storm patterns*

524 Based on stratigraphic data regarding variations in marine benthic  $\delta^{18}\text{O}$  isotopes,  
525 related models for reconstruction of mean sea-surface temperatures, and sea-level  
526 variations pegged to ice-sheet models cited by De Boer et al. (2012, their fig. 1), the  
527 Middle Miocene Climatic Optimum (MMCO) stands out among major climatic shifts  
528 during the last 34 million years. Termination of this phase coincides with expansion of  
529 the East Antarctic Ice Sheet corresponding to distinct pulses dated to 13.8 and 13.2 Ma

1  
2  
3  
4  
5  
6  
7  
8  
9  
10  
11  
12  
13  
14  
15  
16  
17  
18  
19  
20  
21  
22  
23  
24  
25  
26  
27  
28  
29  
30  
31  
32  
33  
34  
35  
36  
37  
38  
39  
40  
41  
42  
43  
44  
45  
46  
47  
48  
49  
50  
51  
52  
53  
54  
55  
56  
57  
58  
59  
60  
61  
62  
63  
64  
65

530 (Westerhold et al., 2005). Global temperatures not only began to receded with the  
531 decline of the MMCO, but evidence from places as distant as the South China Sea and  
532 the Mediterranean Sea suggests that the Intertropical Convergence Zone (ITCZ) was  
533 pushed substantially northward from a position near the equator (John et al., 2003;  
534 Holbourn et al., 2010).

535 A displaced ITCZ could be expected to have a profound effect on climate in the  
536 developing Macaronesian archipelagos of the eastern North Atlantic, including the Cape  
537 Verde islands. In place of steady trade winds that normally arrive from the northeast, the  
538 flow of winds would shift to blow from the southeast. More typical of trade winds in the  
539 Southern Hemisphere, these would brush locally parallel to the West African coast and be  
540 more likely to stimulate sustained marine upwelling. More significant, the northward  
541 migration of the ITCZ should alter the general staging area and subsequent storm tracks  
542 of hurricanes in the North Atlantic. This scenario was employed to account for the  
543 occurrence of major storm deposits formed by Middle Miocene rhodoliths at Cabeço das  
544 Laranjas on Ilhéu de Cima off Porto Santo in the Madeira archipelago (Johnson et al.,  
545 2011). ~~The same post-MMCO scenario also accommodates the preservation of an *in situ*~~  
546 ~~rhodolith field along a sheltered palaeoshore at Pedra de Água on Ilhéu de Cima (Santos~~  
547 ~~et al., 2012).~~

548 Emerging Northern Hemisphere glaciations that intensified through post-Miocene  
549 times served to re-balance the ITCZ and facilitate its return to regions around the equator.  
550 A stable isotope study based on stratigraphy from the southeastern Atlantic (Vidal et al.,  
551 2002) shows a rapid decrease in  $\delta^{18}\text{O}$  values consistent with a general warming trend in  
552 that part of the world already by Messinian time during the Late Miocene. Such a result



1  
2  
3  
4  
5  
6  
7  
8  
9  
10  
11  
12  
13  
14  
15  
16  
17  
18  
19  
20  
21  
22  
23  
24  
25  
26  
27  
28  
29  
30  
31  
32  
33  
34  
35  
36  
37  
38  
39  
40  
41  
42  
43  
44  
45  
46  
47  
48  
49  
50  
51  
52  
53  
54  
55  
56  
57  
58  
59  
60  
61  
62  
63  
64  
65

553 suggests that a scenario **similar to** ~~more in keeping with~~ today's pattern of strong  
554 northeasterly trade winds across the Maraconesian realm, including the Cape Verde  
555 archipelago, was in effect by the end of the Miocene. Hence, present-day climate  
556 patterns dominated by persistent trade winds from the northeast against the island of São  
557 Nicolau (Brand, 2011) should serve as a reliable guide for comparison of windward and  
558 leeward coastal deposits of Late Miocene and Pliocene age around the island. ~~It is~~  
559 ~~noteworthy that wave refraction from wind-driven waves along the eastern shores of~~  
560 ~~Cape Verdian islands like Santiago are fully capable of transporting rhodoliths to the~~  
561 ~~southeast flank, as shown by Pleistocene strata with abundant rhodoliths near Praia~~  
562 ~~(Johnson et al., 2012). Likewise, it is notable from the Pleistocene record that northeast~~  
563 ~~trade winds and local variations caused by topographic baffles are capable of delivering~~  
564 ~~dune sand with extensive rhodolith detritus to the eastern and southeastern shores of Cape~~  
565 ~~Verdean islands (Johnson et al., 2013).~~

566

567 *5.4. Use of volcanic sequences to gauge absolute water depth*

568 Effusive coastal volcanic **successions** ~~sequences~~ such as those resulting from the  
569 extrusion of lava-fed deltas provide **additional** ~~excellent~~ constraints on coeval sea level  
570 and consequently on paleo-water depths of bottomset sediments (Porebski **and**  
571 Gradzinski, 1990; Ramalho, 2011; Johnson et al., 2012; Meireles et al., ~~in press~~ **2013**).  
572 During low- to moderate- effusion rates (**Ramalho et al., 2013**), lava flows entering the  
573 sea typically form structures similar to Gilbert-type deltas, with foresets of pillow lavas  
574 and hyaloclastites overlain by a topset of subaerial lavas; the passage zone between these  
575 two components of the delta thus marks very accurately contemporaneous sea level

1  
2  
3  
4  
5  
6  
7  
8  
9  
10  
11  
12  
13  
14  
15  
16  
17  
18  
19  
20  
21  
22  
23  
24  
25  
26  
27  
28  
29  
30  
31  
32  
33  
34  
35  
36  
37  
38  
39  
40  
41  
42  
43  
44  
45  
46  
47  
48  
49  
50  
51  
52  
53  
54  
55  
56  
57  
58  
59  
60  
61  
62  
63  
64  
65

576 (Porebski & Gradzinski, 1990; Ramalho, 2011). The vertical distance between the  
577 sedimentary bottomset (typically corresponding to marine sediments coeval of the  
578 eruption) and the passage zone, along the dip of the foresets, is thus a reliable way of  
579 estimating the palaeo-water depth of the sediments (Ramalho, 2011; Johnson et al., 2012;  
580 Meireles et al., ~~in press~~ 2013).

581 At Castilhano (Fig. 3), a typical lava delta ~~sequence~~ **succession** with foresets of  
582 pillow lavas and hyaloclastites overly the marine sediments and the passage zone  
583 between overlying submarine and subaerial basalt occurs 25 m above the top of the  
584 limestone, pinpointing coeval stage of sea level around 5.09 Ma (Ramalho et al., 2010b).  
585 At Bodela (Fig. 3), the sedimentary sequence is overlain by massive submarine flows,  
586 and the passage zone between overlying submarine and subaerial basalt occurs 35 m  
587 above the top of the limestone in the Bodela section, suggesting a slightly deeper  
588 deposition than at Castilhano. Farther south at **Baía dos Barreiros** ~~Ponta Barroso~~, the  
589 passage zone is 95 m above the Upper Miocene limestone (Ramalho et al., 2010a),  
590 marking the terminal depth of that limestone as much deeper. **At this locality, however,**  
591 **the value should be treated with caution, because an unconformity marked by a truncated**  
592 **dike occurs between the sediments and overlying lava flows.** For these three localities,  
593 the passage zone **between subaerial and submarine lava flows is coeval and** signifies the  
594 same relative sea level now ~~uplifted~~ **marked** 100 m above ~~the~~ present sea level.  
595 Measurements of accommodated water depth at the time carbonate deposition ceased at  
596 Castilhano, Bodela, and **Baía dos Barreiros** ~~Barroso~~ in the Late Miocene agree reasonably  
597 well with fossil content.

1  
2  
3  
4  
5  
6  
7  
8  
9  
10  
11  
12  
13  
14  
15  
16  
17  
18  
19  
20  
21  
22  
23  
24  
25  
26  
27  
28  
29  
30  
31  
32  
33  
34  
35  
36  
37  
38  
39  
40  
41  
42  
43  
44  
45  
46  
47  
48  
49  
50  
51  
52  
53  
54  
55  
56  
57  
58  
59  
60  
61  
62  
63  
64  
65

598 At Ribeira da Ponta da Pataca on the south-central coast, the observable passage  
599 zone in volcanics overlying Pliocene sedimentary strata is approximately 90 m above  
600 present-day sea level, indicating a possible coeval water column of 35 to 40 m for Pataca  
601 2 (Fig. 7) and 60 to 70 m for Pataca 1 (Fig. 6). The difference in paleo-water depth at  
602 these two localities is an artifact of the natural slope on the Pliocene sea floor. Because  
603 the capping volcanic sequence shared by the two sections consists of a pile of low-angle  
604 submarine sheet flows, there may have been a time lapse between the moment of burial  
605 and the transition to subaerial flows at the passage zone above. Other possible  
606 disconformities may be hidden in the covered interval between the sedimentary strata and  
607 subaerial basalt. A hiatus of any duration may mask an intermittent rise in sea level. In  
608 any case, the *Skolithos* trace fossils at the top of Pataca 1 (Fig. 6) typically reflect a water  
609 depth shallower than suggested by the overlying passage zone. At Portinho da Mulher  
610 Branca near Praia on Santiago island, for example, *Skolithos* was related to an overlying  
611 passage zone indicating a water depth of only 12 to 15 m (Johnson et al., 2012). This  
612 discrepancy in conflicting water-depth indicators remains to be resolved either by  
613 extending the bathymetric range of the ichnofossil or by an obfuscating time gap.

614

615 **6. Conclusions**

616 Examples of contrasting windward and leeward settings from paleoislands are  
617 well documented, but mainly from continental shelves. The distribution and fossil  
618 content of surviving Upper Miocene limestone strata on São Nicolau are limited but  
619 adequate to outline patterns in intertidal to shallow, sub-tidal biofacies marine biotas in  
620 close proximity to rocky shores influenced by winds and waves around one of the

1  
2  
3  
4  
5  
6  
7  
8  
9  
10  
11  
12  
13  
14  
15  
16  
17  
18  
19  
20  
21  
22  
23  
24  
25  
26  
27  
28  
29  
30  
31  
32  
33  
34  
35  
36  
37  
38  
39  
40  
41  
42  
43  
44  
45  
46  
47  
48  
49  
50  
51  
52  
53  
54  
55  
56  
57  
58  
59  
60  
61  
62  
63  
64  
65

621 windward volcanic islands in the Cape Verde Archipelago. Supplementary data from a  
622 comparatively thick Pliocene **succession** sequence on the island's south-central shore  
623 provide further insight on the potential richness achieved by **biofacies** in a setting better  
624 sheltered from wave shock. Four core conclusions highlight the results of this study. ~~with~~  
625 ~~regard to marine life on the margins of a volcanically active oceanic island.~~

1. Limestone dominated by whole rhodoliths follows a distinct band correlated from  
the oasis at Castilhano to the canyon of the Ribeira de Covoada de Bodela on the  
northeast flank of São Nicolau. Relatively small in size, the rhodoliths were  
swept shoreward from a shallow bank situated nearby to the north or northeast.  
Many are nucleated around basalt pebbles eroded from an adjacent rocky shore.  
These ~~spherical~~ algal concretions accumulated in vast numbers as a transported  
assemblage deposited against the rocky shore, even pressed below overhangs in  
the **bedrock basalt**. Although poor in calcareous nannofossils, the identified  
assemblage is compatible with a Late Miocene (Messinian) assignment. ~~This~~  
~~result is in rough agreement with the 5.09±0.07 Ma age determined by Ramalho~~  
~~et al. (2010b) for the pillow lavas immediately above.~~

2. Whole rhodoliths are absent from the coeval limestone at Baía dos Barreiros in  
southeast São Nicolau **but extensive rhodolith sand is well developed as cliniform**  
**structures dipping seaward to the south. The more loosely equivalent limestone at**  
**Monte Focinho near the island's south-central shore also includes fine debris of**  
**coralline red algae mixed with crushed barnacles.** A more sandy limestone  
deposit of Pliocene age at Ribeira da Ponta da Pataca on the south-central coast of  
São Nicolau includes elements such as the whole (and broken) valves of pectinid

1  
2  
3  
4  
5  
6  
7  
8  
9  
10  
11  
12  
13  
14  
15  
16  
17  
18  
19  
20  
21  
22  
23  
24  
25  
26  
27  
28  
29  
30  
31  
32  
33  
34  
35  
36  
37  
38  
39  
40  
41  
42  
43  
44  
45  
46  
47  
48  
49  
50  
51  
52  
53  
54  
55  
56  
57  
58  
59  
60  
61  
62  
63  
64  
65

644 bivalves, as well as whole branches of the *Porites* coral and delicate  
645 *Thalamoporella* bryozoan that are unusual or entirely absent from deposits on the  
646 north side of the island. A Pliocene age for the Pataca deposits based on  
647 calcareous nannofossils concurs with the age of basaltic lavas near the overlying  
648 passage zone dated at 3.06±0.17 Ma.

3. With a change after the Middle Miocene Climatic Optimum that brought the  
Intertropical Convergence Zone closer to the equator, the Late Miocene and  
Pliocene conditions at São Nicolau experienced steady winds from the northeast  
that generated ocean swell. Although smaller than today by perhaps 40%, the  
Late Miocene island still presented a long east-west oriented northern shore that  
felt the full impact of these conditions, much as today. Thus, the fossil deposits at  
Castilhano and Bodela represent accumulations on an exposed, windward coast,  
while those at **Baía dos Barreiros and** Pataca are indicative of a more sheltered,  
leeward coast.

4. Upper Miocene limestone beds near the northeastern coast at Castilhano and  
Bodela are overlain by submarine flows with passage zones to subaerial flows at  
intervals 25 m and 35 m above, respectively. Marine onlap of the carbonates  
concluded at those water depths with no discrepancy indicated by fossil content.  
Certain discrepancies with **unconformities and** trace fossils remain to be solved,  
as **in the southern successions** ~~the Pliocene Pataca sequence~~. Overall, however,  
the application of such transitions in volcanic flows to measure original water  
depth is a useful technique in the reconstruction of coastal conditions.

1  
2  
3  
4 **667 Acknowledgments**

5  
6 668 This study was funded under grant CGL2010-15372-BTE from the Spanish  
7  
8  
9 669 Ministry of Science and Innovation to project leader Eduardo Mayoral (University of  
10  
11 670 Huelva). Support from Research Group RNM276 also is acknowledged. Extra support  
12  
13  
14 671 for work on calcareous nannofossils came from PTDC/MAR/102800/2008. R. Ramalho  
15  
16 672 was funded by an FP7-PEOPLE-2011-IOF Marie Curie Postdoctoral Fellowship, which  
17  
18  
19 673 is gratefully acknowledged. We thank Dr. Björn Berning (Upper Austrian State  
20  
21 674 Museum, Leonding, Austria) for identification of the Pataca bryozonas to genus level and  
22  
23  
24 675 Dr. Davide Bassi (Department of Earth Sciences, Ferrara University, Italy) for  
25  
26 676 identification of the Castilhano rhodoliths to genus level. The editor and two anonymous  
27  
28  
29 677 reviewers provided useful comments that helped to improve the final manuscript.  
30

31 678

32  
33 **679 References**

34  
35  
36 680 Ávila, S., Ramalho, R.S., Vullo, R., 2012. Systematics, palaeoecology and palaeo-  
37  
38 681 biogeography of the neogene fossil sharks from the Azores (Northeast Atlantic).  
39  
40  
41 682 *Annales de Paléontologie* 98, 167–189.  
42  
43 683 Amen, R.G., Neto, A.I, Azevedo, J.M.N., 2005. Coralline-algal framework in the  
44  
45 684 Quaternary of Prainha (Santa Maria Island, Azores). *Revista Española de*  
46  
47  
48 685 *Micropaleontologia* 37, 63–70.  
49  
50  
51 686 Baarli, B.G., Cachão, M., Silva, C.M. da, Johnson, M.E., Mayoral, E.J., Santos, A., 2013.  
52  
53 687 A Middle Miocene carbonate embankment on an active volcanic slope: Ilhéu de  
54  
55 688 Baixo, Madeira Archipelago, Eastern Atlantic. *Geological Journal*, in press DOI:  
56  
57  
58 689 10.1002/gj.2513.  
59  
60  
61  
62  
63  
64  
65

1  
2  
3  
4  
5  
6  
7  
8  
9  
10  
11  
12  
13  
14  
15  
16  
17  
18  
19  
20  
21  
22  
23  
24  
25  
26  
27  
28  
29  
30  
31  
32  
33  
34  
35  
36  
37  
38  
39  
40  
41  
42  
43  
44  
45  
46  
47  
48  
49  
50  
51  
52  
53  
54  
55  
56  
57  
58  
59  
60  
61  
62  
63  
64  
65

690 Bebiano, J., 1932. A geologia do Arquipélago de Cabo Verde. Comunicações dos  
691 Serviços Geológicos de Portugal 18, 167–187.

692 Bernoulli, D., Hottinger, L., Spezzaferri, S., Stille, P. 2007. Miocene shallow-water  
693 limestone from São Nicolau (Cabo Verde): Caribbean-type benthic fauna and time  
694 constraints for volcanism. Swiss Journal of Geosciences 100, 215–225.

695 Braga, J.C., Bassi, D., Piller, W.E., 2010. Palaeoenvironmental significance of  
696 Oligocene-Miocene coralline red algae - a review. In Mutti, M, Piller, W.E.,  
697 Betzler, C. (eds.), Carbonate Systems During the Oligocene-Miocene Climatic  
698 Transition. International Association of Sedimentologists, Spec. Publ., 42, 165–182.

699 Bosence, D., 1976. Ecological studies on two unattached coralline algae from western  
700 Ireland. Palaeontology 19, 71–88.

701 Bosence, D.K.J., 1983. The occurrence and ecology of Recent rhodoliths -a review. In:  
702 Peryt, T.M. (Ed.), Coated Grains. Springer-Verlag, Berlin, pp. 217–224.

703 Bown, P., 1998. Calcareous Nannofossil Biostratigraphy. Chapman and Hall, Dordrecht,  
704 The Netherlands, 314 p.

705 Brand, S. (Editor), African severe weather port guide from Naval Research Laboratory in  
706 Monterey, California, last modified April 2011.  
707 [http://www.nrlmry.navy.mil/port\\_studies/africaports/Mindelo/index.html](http://www.nrlmry.navy.mil/port_studies/africaports/Mindelo/index.html);

708 De Boer, B., Van de Wal, R.S.W., Lourens, L.J., and Bintanja, R., 2012. Transient nature  
709 of the Earth's climate and the implications for the interpretation of benthic  $\delta^{18}\text{O}$   
710 records. Palaeogeography, Palaeoclimatology, Palaeoecology 335–336, 4–11.

711 Dollar, S.J., Tribble, G.W., 1993. Recurrent storm disturbance and recovery: a long-term  
712 study of coral communities in Hawaii. Coral Reefs 12, 223–233.

1  
2  
3  
4  
5  
6  
7  
8  
9  
10  
11  
12  
13  
14  
15  
16  
17  
18  
19  
20  
21  
22  
23  
24  
25  
26  
27  
28  
29  
30  
31  
32  
33  
34  
35  
36  
37  
38  
39  
40  
41  
42  
43  
44  
45  
46  
47  
48  
49  
50  
51  
52  
53  
54  
55  
56  
57  
58  
59  
60  
61  
62  
63  
64  
65

713 Dott, R.H., Jr. 1974. Cambrian tropical storm waves in Wisconsin. *Geology* 2, 243–  
714 246.

715 Duprat, H.I., Friss, J., Holm, P.M., Grandvoinet, T., Sørensen, R.V. 2007. The volcanic  
716 and geochemical development of São Nicolau, Cape Verde Islands: Constraints  
717 from field and  $^{40}\text{Ar}/^{39}\text{Ar}$  evidence. *Journal of Volcanology and Geothermal*  
718 *Research* 162, 1–19.

719 Halfar, J., Mutti, M., 2005. Global dominance of coralline red-algal facies: A response to  
720 Miocene oceanographic events. *Geology* 33, 481–484.

721 Holbourn, A., Kuhnt, W., Regenberg, M., Schulz, M., Mix, A., Andersen, N., 2010. Does  
722 Antarctic glaciation force migration of the tropical rain belt? *Geology* 38, 783–786.

723 John, C.M., Mutti, M., Adatte, T., 2003. Mixed carbonate-siliciclastic record on the  
724 North African margin (Malta) – coupling of weathering processes and mid Miocene  
725 climate. *Geological Society of America Bulletin* 115, 217–229.

726 Johnson, M.E., 2002. Paleoislands in the stream: paleogeography and expected  
727 circulation patterns. In: Monegatti, P. Cecca, F. and Raffi, S. (eds.): *International*  
728 *Conference “Paleobiogeography & Paleoecology 2001”*, Piacenza and Castell’  
729 *Arquato 2001. Geobios*, v. 35 (Mémoire Spécial No. 24), pp. 96-106.

730 Johnson, M.E., Baarli, B.G., 2012. Development of intertidal biotas through Phanerozoic  
731 time. In: Talent, J.A. (ed), *Earth and Life, International Year of Planet Earth*,  
732 *Springer Science+Business Media B.V.*, pp. 63–128.

733 ~~Johnson, M.E., Hayes, M.L., 1993. Dichotomous facies on a Late Cretaceous rocky~~  
734 ~~island as related to wind and wave patterns (Baja California, Mexico). *Palaios* 8,~~  
735 ~~385–395.~~



1  
2  
3  
4  
5  
6  
7  
8  
9  
10  
11  
12  
13  
14  
15  
16  
17  
18  
19  
20  
21  
22  
23  
24  
25  
26  
27  
28  
29  
30  
31  
32  
33  
34  
35  
36  
37  
38  
39  
40  
41  
42  
43  
44  
45  
46  
47  
48  
49  
50  
51  
52  
53  
54  
55  
56  
57  
58  
59  
60  
61  
62  
63  
64  
65

736 ~~Johnson, M.E., Baarli, G.B., Silva, C.M. da, Cachão, M., Ramalho, R.S., Ledesma-~~  
737 ~~Vázquez, J., Mayoral, E.J., and Santos, A., 2013. Coastal dunes with high content~~  
738 ~~of rhodolith (coralline red algae) bioclasts: Pleistocene formations on Maio and São~~  
739 ~~Nicolau in the Cape Verde archipelago. Aeolian Research 8, 1–9.~~

740 Johnson, M.E., Baarli, B.C., Cachão, M., Silva, C.M. da, Ledesma-Vázquez, J., Mayoral,  
741 E.J., Ramalho, R.S., and Santos, A., 2012. Rhodoliths, uniformitarianism, and  
742 Darwin: Pleistocene and Recent carbonate deposits in the Cape Verde and Canary  
743 archipelagos. *Palaeogeography, Palaeoclimatology, Palaeoecology* 329–330, 83–  
744 100.

745 Johnson, M.E., Silva, C.M. da, Santos, A., Baarli, B.G., Cachão, M., Mayoral, E.J.,  
746 Rebelo, A.C., Ledesma-Vázques, J., 2011. Rhodolith transport and immobilization  
747 on a volcanically active rocky shore: Middle Miocene at Cabeço das Laranjas on  
748 Ilhéu de Cima (Madeira Archipelago, Portugal). *Palaeogeography,*  
749 *Palaeoclimatology, Palaeoecology* 300, 113–127.

750 Littler, M.M., Littler, D.S., Murray, S.N., Seaph R.R., 1991. Southern California rocky  
751 intertidal ecosystems. In: Matheison, A.C., Nienhuis, P.H. (eds.), *Intertidal and*  
752 *Litoral Ecosystems. Ecosystems of the World* 24, Elsevier, Amsterdam, pp. 273–  
753 296.

754 MacArthur, R.H., 1972. *Geographical Ecology*. Harper and Row, Publishers, New York,  
755 269 pp.

756 Macedo, J.R., Serralheiro, A., Silva, L.C., 1988. Notícia explicativa da carta da ilha de S.  
757 Nicolau (Cabo Verde) na escala de 1:50 000. *Garcia de Orta, Série Geologia* 11, 1–  
758 32.

1  
2  
3  
4  
5  
6  
7  
8  
9  
10  
11  
12  
13  
14  
15  
16  
17  
18  
19  
20  
21  
22  
23  
24  
25  
26  
27  
28  
29  
30  
31  
32  
33  
34  
35  
36  
37  
38  
39  
40  
41  
42  
43  
44  
45  
46  
47  
48  
49  
50  
51  
52  
53  
54  
55  
56  
57  
58  
59  
60  
61  
62  
63  
64  
65

759 Mayoral, E., Ledesma-Vázquez, J., Baarli, B.G., Santos, A., Ramalho, R., Cachão, M.,  
760 Silva, C.M. da, Johnson, M.E., 2013. Ichnology in ocean islands; case studies from  
761 the Cape Verde Archipelago. *Palaeogeography, Palaeoclimatology, Palaeoecology*  
762 381–382, 47–66.

763 McNutt, M., 1988. Thermal and mechanical properties of the Cape Verde Rise. *Journal of*  
764 *Geophysical Research (Solid Earth)* 93(B4), 2784–2794.

765 Meireles, R.P., Quartau, R., Ramalho, R.S., Rebelo, A.C., Madeira, J., Zanon, V., Ávila,  
766 S.P., 2013. Depositional processes on oceanic island shelves—evidence from storm-  
767 generated Neogene deposits from the mid-North Atlantic. *Sedimentology* 60, 1769–  
768 1785.

769 Menard, H.W, 1986. *Islands*. Scientific American Library, New York, 219 p.

770 Mitchell-Thomé, R.C., 1972. Outline of the geology of the Cape Verde Archipelago.  
771 *Geologische Rundschau* 61, 1087–1109.

772 Perch-Nielsen, K., 1985. Cenozoic calcareous nannofossils. In: Bolli, H.H., Saunders,  
773 J.B., Perch-Nielsen, K. (eds.), *Plankton Stratigraphy, Volume 1* (2<sup>nd</sup> edition),  
774 Cambridge Earth Science Series, pp. 329–554.

775 Porebski, S., Gradzinski, R., 1990. Lava-fed Gilbert-type delta in the Polonez Cove  
776 Formation (Lower Oligocene), King George Island, West Antarctica. In: Colella, A.  
777 and Prior, D. (eds), *Coarse Grained Deltas*, International Association of  
778 Sedimentologists Special Publication 10, 335–351.

779 Ramalho, R.S. 2011. *Building the Cape Verde Islands*. Springer, 1<sup>st</sup> Edition, 207 p.

780 Ramalho, R.S., Quartau, R., Trenhaile, A.S., Mitchell, N.C., Woodroffe, C.D., Ávila,  
781 S.P., 2013. *Coastal evolution on volcanic oceanic islands: a complex interplay*

1  
2  
3  
4  
5  
6  
7  
8  
9  
10  
11  
12  
13  
14  
15  
16  
17  
18  
19  
20  
21  
22  
23  
24  
25  
26  
27  
28  
29  
30  
31  
32  
33  
34  
35  
36  
37  
38  
39  
40  
41  
42  
43  
44  
45  
46  
47  
48  
49  
50  
51  
52  
53  
54  
55  
56  
57  
58  
59  
60  
61  
62  
63  
64  
65

782            **between volcanism, erosion, sedimentation, sea level change and biogenic**  
783            **production. *Earth Science Reviews* 127, 140–170.**

784    Ramalho, R.S., Helffrich, G., Vance, D., Schmidt, D.N., 2010a. Tracers of uplift and  
785            subsidence in the Cape Verde Archipelago. *Journal of the Geological Society* 167,  
786            519–538.

787    Ramalho, R.S., Helffrich, G., Cosca, M., Vance, D., Hofmann, D., Schmidt, D.N., 2010b.  
788            Vertical movements of ocean island volcanoes: Insights from a stationary plate  
789            environment. *Marine Geology* 275, 84–95.

790    Ramalho, R.S., Helffrich, G., Cosca, M., Vance, D., Hofmann, D., Schmidt, D.N., 2010c.  
791            Episodic swell growth inferred from variable uplift of the Cape Verde hotspot  
792            islands. *Nature Geoscience* 3(11), 774–777.

793    Robertson, A.H.F., 1984. Mesozoic deep-water and Tertiary volcanoclastic deposition of  
794            Maio, Cape Verde Islands: Implications for Atlantic paleoenvironments and ocean  
795            island volcanism. *Geological Society of America Bulletin* 94, 433–453.

796    ~~Rong, J., Johnson, M.E., Deng, Z., Dong, D., Xue, Y., Baarli, B.G., Wang, G., 2013.~~  
797            ~~Coral stromatoporoid faunas from the shores of an Upper Silurian island, Inner~~  
798            ~~Mongolia, North China. *Association of Australasian Palaeontologists Memoir* 40, 95–~~  
799            ~~105.~~

800    Santos, E., Mayoral, E.J., Silva, C.M. da, Cachão, M., Johnson, M.E., Baarli, B.G., 2011.  
801            Miocene intertidal zonation on a volcanically active shoreline: Porto Santo in the  
802            Madeira Archipelago, Portugal. *Lethaia* 44, 26–32.

803    Santos, A.G., Mayoral, E., Johnson, M.E., Baarli, B.G., Silva, C.M. da, Cachão, M.,  
804            Ledesma-Vázquez, J., 2012. Basalt mounds and adjacent depressions attract

1  
2  
3  
4  
5  
6  
7  
8  
9  
10  
11  
12  
13  
14  
15  
16  
17  
18  
19  
20  
21  
22  
23  
24  
25  
26  
27  
28  
29  
30  
31  
32  
33  
34  
35  
36  
37  
38  
39  
40  
41  
42  
43  
44  
45  
46  
47  
48  
49  
50  
51  
52  
53  
54  
55  
56  
57  
58  
59  
60  
61  
62  
63  
64  
65

805 contrasting biofacies on a volcanically active Middle Miocene shoreline (Porto  
806 Santo, Madeira Archipelago, Portugal). *Facies* 58, 573–585.

807 Serralheiro, A., Ubaldo, M., 1979. Estudo estratigráfico dos sedimentos do Campo da  
808 Preguiça ilha de S. Nicolau (Cabo Verde). *Garcia de Orta, Série Geologia* 3(1-2),  
809 75–82.

810 Sneed, E.D., Folk, R.L., 1958. Pebbles in the lower Colorado River, Texas, a study in  
811 particle morphogenesis. *Journal of Geology* 66, 114–150.

812 Steiner, C., Hobson, A., Favre, P., Stampfli, G.M., Hernandez, J., 1998. Mesozoic  
813 sequence of Fuerteventura (Canary Islands): Witness of early Jurassic sea-floor  
814 spreading in the central Atlantic. *Geological Society of America Bulletin* 110,  
815 1304–1317.

816 Torres, A., Soares, J., 1946. *Formações Sedimentares do Arquipélago de Cabo Verde. I -*  
817 *Actualização de conhecimentos. Junta das Missões Geográficas e de Investigações*  
818 *Coloniais*, 398 p.

819 Vidal, L., Bickert, T., Wefer, G., and Röhl, U., 2002. Late Miocene stable isotope  
820 stratigraphy of SE Atlantic ODP Site 1085: Relation to Messinian events. *Marine*  
821 *Geology* 180, 71–85.

822 Westerhold, T., Bickert, T., Röhl, U., 2005. Middle to late Miocene oxygen isotope  
823 stratigraphy of ODP site 1085 (SE Atlantic): new constrains on Miocene climate  
824 variability and sea-level fluctuations. *Palaeogeography, Palaeoclimatology,*  
825 *Palaeoecology* 217, 205–222.

826 Zazo, C., Goy, J.L., Hillaire-Marcel, C., Gillot, P.Y., Soler, V., González, J.H., Dabrio,  
827 C.J., Ghaleb, B., 2002. Raised marine sequences of Lanzarote and Fuerteventura

1  
2  
3  
4  
5  
6  
7  
8  
9  
10  
11  
12  
13  
14  
15  
16  
17  
18  
19  
20  
21  
22  
23  
24  
25  
26  
27  
28  
29  
30  
31  
32  
33  
34  
35  
36  
37  
38  
39  
40  
41  
42  
43  
44  
45  
46  
47  
48  
49  
50  
51  
52  
53  
54  
55  
56  
57  
58  
59  
60  
61  
62  
63  
64  
65

828 revisited – a reappraisal of relative sea-level changes and vertical movements in the  
829 eastern Canary Islands during the Quaternary. *Quaternary Science Reviews* 21,  
830 2019–2046.

831

832 **Figure Captions**

833 **Fig. 1.** Maps at various scales for the North Atlantic archipelagos of Macaronesia with  
834 details shown for the Cape Verde archipelago and the island of São Nicolau.

835 **Fig. 2.** Reconstruction of São Nicolau during the Late Miocene at ~5.1 Ma.

836 **Fig. 3.** Stratigraphic profiles for localities at Castilhano and Ribeira de Covoada de  
837 Bodela on the northeast flank of Miocene São Nicolau.

838 **Fig. 4.** Upper Miocene deposits against basalt unconformities from the northeast part of  
839 São Nicolau showing details of faunal components: A) Irregular unconformity surface  
840 overlain by abundant rhodoliths at Castilhano (figure at right for scale), B) Small  
841 overhang of basalt filled with rhodolith limestone, C) Part of a basalt boulder above the  
842 unconformity surface with dwelling structures formed by regular echinoids assigned to  
843 the trace fossil *Circolites kotoncensis*, D) Trace fossil *Thalassinoides suevicus* from mid-  
844 section at Castilhano (see Fig. 3), E) Typical interval packed with rhodoliths many of  
845 which formed around basalt pebbles (arrows), and F) Basal conglomerate and overlying  
846 rhodolith limestone at Ribeira de Covoada de Bodela (figure at left for scale).

847 **Fig. 5.** Triangular plots showing the relative shapes of fossil rhodoliths: A, from the  
848 lower part of the section at Castilhano, B) from the middle part of the section at  
849 Castilhano, and C) from the lower part of the section at Bodela.

1  
2  
3  
4  
5  
6  
7  
8  
9  
10  
11  
12  
13  
14  
15  
16  
17  
18  
19  
20  
21  
22  
23  
24  
25  
26  
27  
28  
29  
30  
31  
32  
33  
34  
35  
36  
37  
38  
39  
40  
41  
42  
43  
44  
45  
46  
47  
48  
49  
50  
51  
52  
53  
54  
55  
56  
57  
58  
59  
60  
61  
62  
63  
64  
65

850 **Fig. 6.** Stratigraphic profile for the sequence at Baía dos Barreiros on the southeast flank  
851 of Miocene São Nicolau.

852 **Fig. 7.** Stratigraphic profile for the Pliocene coastal sequence at Ribeira da Ponta Pataca  
853 on the southwest flank of Miocene São Nicolau.

854 **Fig. 8.** Stratigraphic profile for the more inland Pliocene sequence at Pataca 2.

855 **Fig. 9.** Pliocene deposits capped by basalt from the southwest coast of São Nicolau at  
856 Ribeira da Pataca: A) Outcrop overview of Pataca 1 (see Fig. 7), B) Cluster of the coral  
857 *Porites* sp. from the lower beds, C) Ramose bryozoan *Thalamoporella* sp. from the lower  
858 beds, D) Disarticulated shells, mostly *Argopecten* aff. *flabellum* from the upper beds, E)  
859 Trace fossil *Skolithos linearis* from the top of the section, F) Outcrop overview of the  
860 Pataca 2 section (see Fig. 8), and G) Coral colonies of *Tubastrea* sp. bored by pholad  
861 bivalves from the middle of the section.

- Late Miocene São Nicolau Island was impacted by NE trade winds as today.
- Windward biofacies are rich in rhodoliths nucleated on eroded basalt pebbles.
- Shape analysis of abundant rhodoliths shows selection for transported forms.
- Leeward biofacies are dominated by sand from crushed rhodoliths.
- Nannofossils, indicate L. Miocene Messinian and Pliocene ages for studied strata.
- Passage zone from submarine to subaerial flows tests the water depth for overlapped paleoshores.

Editor: *Palaeogeography, Palaeoclimatology, Palaeoecology*

Dear Editor Surlyk,

On behalf of my co-authors, I am re-submitting our manuscript "Miocene-Pliocene rocky shores on São Nicolau (Cape Verde Islands): Contrasting windward and leeward biofacies on a volcanically active oceanic island" for your reconsideration.

You will find all our new materials in good order, include a clean copy of the revised text, a copy showing where all changes have been made, and the detailed revision notes. The most significant addition to our study is a new stratigraphic profile from a strategic location on the SE flank of Sao Nicolau (new Fig. 6). All your suggestions regarding editorial changes have been made. Reviewer #1 offered only a brief report that chiefly asked for a better discussion on the repercussions of our rhodolith shape analyses (Fig. 5) for the discussion section, which we have done. Reviewer #2 has a high regard for the 2010 paper by Braga et al. That paper sets out certain predictions regarding the depth preference of rhodoliths by genera. We have taken pains to incorporate this paper into our ms. and to present new data on generic identifications from our São Nicolau collections –as well as to summarize the generic identifications previously reported in some of our earlier rhodolith studies in the Canary and Madeira islands.

We are a large group, but our contribution represents the confluence of several different areas of expertise by the various participants that range from interests in former rocky shores and coastal geomorphology to palaeogeography to nannofossil biostratigraphy to the intersection of rhodolith taphonomy and trace fossils. A novel aspect of our work involves use of the passage zone from submarine to subaerial flows that bury limestone deposits on a volcanic island as a meter-stick to gauge absolute water depth at the moment of local extinction.

A growing literature exists on the burial and exhumation of entire "fossil" islands from the geologic record. By far, most of the existing examples come from continental islands, some of which include evidence of windward/leeward relationships defined on the basis of sedimentological and paleontological criteria. Our contribution is one of the very few to consider the dynamics on oceanic, volcanic islands from the past.

All co-authors contributed to the revision of this paper and all gave their approval for the version now submitted for re-evaluation.

Respectfully,

Markes E. Johnson  
December 6, 2013



1 *Palaeogeography, Palaeoclimatology, Palaeoecology*

2

3 Miocene–Pliocene rocky shores on São Nicolau (Cape Verde Islands): Contrasting  
4 windward and leeward biofacies on a volcanically active oceanic island

5

6 Markes E. Johnson<sup>a\*</sup>, Ricardo S. Ramalho<sup>b,c</sup>, B. Gudveig Baarli<sup>a</sup>, Mário Cachão<sup>d</sup>,  
7 Carlos M. da Silva<sup>d</sup>, Eduardo J. Mayorale, and Ana Santosa

8 *a Department of Geosciences, Williams College, Williamstown, MA 01267 USA*

9 *b School of Earth Sciences, University of Bristol, Wills Memorial Building, Queens's  
10 Road, Bristol, BS8 1RJ, UK*

11 *c Lamont-Doherty Earth Observatory at Columbia University, Comer Geochemistry  
12 Building, P.O. Box 1000 Palisades, NY 10964 USA*

13 *c Faculdade de Ciências da Universidade de Lisboa, Departamento de Geologia e  
14 Centro de Geologia, Campo Grande, 1749-016 Lisboa, Portugal*

15 *d Departamento de Geodinámica y Paleontología, Facultad de Ciencias Experimentales,  
16 Universidad de Huelva, Campus de El Carmen, Avda. 3 de Marzo, s/n, 21071 Huelva,  
17 Spain*

18 Corresponding author; E-mail address: [mjohnson@williams.edu](mailto:mjohnson@williams.edu)

19 Department of Geosciences, Williams College, ph (413) 597-2329; fax (413) 597-4116

20

21 ABSTRACT

22 North Atlantic islands in the Cape Verde Archipelago off the coast of West Africa

23 commonly feature an elongated N–S shape in which reduced northern coasts and longer

24 eastern shores absorb the brunt of wave activity and long-shore currents generated by

25 prevailing North East Trade Winds. Located in the middle windward islands, São  
26 Nicolau is unusual in profile with an elongated E–W configuration that offers a broad  
27 target against high-energy, wind-driven waves. Conversely, the south shore of São  
28 Nicolau provides relatively wide shelter in a leeward setting. Reconstruction of the  
29 proto-island prior to the onset of the Main Eruptive stage during the Late Miocene at ~5.1  
30 Ma reveals a moderately smaller island with essentially the same E–W orientation. This  
31 study combines previous data with results from a detailed stratigraphic log based on  
32 Upper Miocene limestone deposits on the island’s south flank for comparison with  
33 stratigraphic profiles of Upper Miocene limestone from the island’s northeast quarter.  
34 Logs from a Pliocene sandy limestone outcropping on the south-central coast of São  
35 Nicolau give added context to the diversity of marine invertebrates, including branching  
36 coral colonies and delicate ramose bryozoans that found shelter in a leeward setting.  
37 Whole rhodoliths contribute the main fabric of carbonates deposited against rocky shores  
38 on the northern, exposed side of the Miocene island, whereas only traces of worn  
39 rhodoliths and rhodolith sand occur as in finer Miocene grainstone on the island’s  
40 southern, protected side. Miocene and Pliocene carbonate deposits were terminated by  
41 submarine flows on an actively growing volcanic island. The passage zone from  
42 submarine to subaerial flows on the island’s flanks makes a useful meter-stick to gauge  
43 absolute water depth at the moment of local extinction by volcanic activity.

44

45 *Keywords:* Coastal deposition, Miocene, Pliocene, Rhodoliths (Rhodophyta), Northeast  
46 Trade Winds, Volcanic islands

47 **1. Introduction**

48 Islands are singular landscapes where the limits of habitability are proportionate  
49 to size and distance from the nearest mainland (MacArthur, 1972). However arrayed in  
50 the seas or oceans that surround them, islands also enforce restrictions on life subject to  
51 the wider field of prevailing winds, ocean currents, storm tracks, and other climatic  
52 factors typical for any given geographic realm. Coral species that colonized the big  
53 island of Hawaii, for example, thrive on the leeward Kona Coast where ocean swell from  
54 the South Pacific is moderate compared to rough conditions on the windward Hamakua  
55 Coast where wave shock energized by persistent trade winds prohibits coral growth  
56 (Dollar and Tribble, 1993). On continental islands closer to a mainland, variations in  
57 physical factors between exposed, outer rocky shores and sheltered inner shores regulate  
58 the distribution of marine organisms, as found for example around the Channel Islands of  
59 southern California (Littler et al., 1991). The geological record is capable of preserving  
60 whole islands that demonstrate fossil evidence for contrasting exposed and sheltered  
61 biotopes (Johnson, 2002). Due to plate tectonics and the re-cycling of oceanic crust, the  
62 geologic record is biased in favor of continental islands leading as far back as the  
63 Cambrian (Dott, 1974). In contrast, hotspot oceanic islands are transient features due to  
64 island subsidence and strong marine erosion. Consequently, their onshore record  
65 typically does not extend beyond Miocene times (Menard, 1986). Their mid-ocean  
66 geography, however, makes them prime localities to look at present and past coastal  
67 biotopes and sedimentary processes in an oceanic setting, as well as places to gain  
68 insights on ancient patterns of wind and ocean currents.

69 All 20 Miocene and 15 Pliocene examples of biotas associated with rocky shores  
70 from localities around the world surveyed by Johnson and Baarli (2012) come from

71 continental shelves. Rocky-shore biotas from oceanic islands, however, are becoming  
72 better known. Santos et al. (2011) described a rocky shore from the Middle Miocene of  
73 Porto Santo in Madeira (Portugal) that features a biota with intertidal zonation.  
74 Additional studies on Miocene carbonates from Porto Santo include those by Johnson et  
75 al. (2011), Santos et al. (2012), and Baarli et al. (2013). The coastal carbonates of Porto  
76 Santo and many other oceanic islands in the northeast Atlantic Ocean often incorporate  
77 whole rhodoliths or sediments eroded from rhodoliths. These coralline red algae are non-  
78 attached and spherical to sub-spherical in shape due to concentric growth accruing with  
79 circumrotary movement in benthic settings under sun-lighted waters. Evidence collected  
80 on a global scale suggests that rhodoliths registered peak domination in carbonate facies  
81 during Early to Middle Miocene times (Halfar and Mutti, 2005; Braga et al., 2010).

82       Island groups from the North Atlantic realm of Macaronesia, which include the  
83 Azores, Madeira (with the Selvagens), Canary, and Cape Verde archipelagos, have a  
84 volcanic history tracing back to the Miocene or older. Additionally, many of the  
85 Macaronesian islands were subjected to uplift, making them particularly rich in exposed  
86 marine sedimentary and volcanic sequences (Ramalho et al., 2010a, b; Ávila et al., 2012;  
87 Meireles et al., 2013). Like Madeira, the fabric of Miocene and younger limestone  
88 deposits from many of the other island groups is enriched by rhodoliths and rhodolith-  
89 derived sediments (Mayoral et al., 2013; Johnson et al., 2012; Amen et al., 2005; Zazo et  
90 al., 2002). A theme of overarching regional interest concerns the degree to which the  
91 strong Northeast Trade Winds pervasive across much of Macaronesia influenced the  
92 formation of rhodolith limestone.

93           This study is focused on São Nicolau, one of the principal windward islands  
94 belonging to the Cape Verde Archipelago in southern Macaronesia off the West African  
95 coast of Senegal. The goal of this study is to test the hypothesis that differences in  
96 biofacies around the margins of the island are due to physical constraints related to  
97 contrasting windward and leeward environments. Two tasks shape the project's  
98 organization: 1) to reconstruct the approximate size and configuration of the proto-island  
99 of São Nicolau during the Late Miocene and immediately before the onset of the Main  
100 Eruptive Complex (after Macedo et al., 1988), and 2) to compile detailed stratigraphic  
101 profiles for Miocene and Pliocene sections that include biofacies associated with former  
102 rocky shores.

103

## 104 **2. Geographic and geologic settings**

### 105 *2.1. Physical geography*

106           São Nicolau is one of 15 volcanic islands in the Cape Verde Archipelago  
107 dispersed over a prominent seafloor anomaly called the Cape Verde Rise (Fig. 1). Due to  
108 an almost-stationary position with respect to its melting source, the archipelago  
109 corresponds to a cluster of islands arrayed in a west-facing semi-arc (McNutt, 1988;  
110 Ramalho, 2011). Traditionally, the archipelago has been classified into windward and  
111 leeward islands with respect to the dominant NE trade winds. São Nicolau is one of the  
112 windward islands and it ranks fifth largest in size with an area of 343 km<sup>2</sup>, which is  
113 slightly above the median compared to the 14 other Cape Verdean islands (Mitchell-  
114 Thomé, 1972). In terms of elevation, São Nicolau is the fourth highest with a maximum  
115 elevation of 1,304 m (Mitchell-Thomé, 1972).

116           The location of São Nicolau within the north-central part of the archipelago and  
117 the island's overall shape make it an appropriate subject for this study. In particular, the  
118 north shore of São Nicolau is unusual for a roughly east–west alignment that extends over  
119 a distance of 45 km (Fig. 1). No other island in the group makes such a broad target for  
120 the steady trade winds arriving out of the northeast. With little difference between winter  
121 and summer seasons, the north shore of São Nicolau is subject to winds that reach 5–6 on  
122 the Beaufort Scale (Brand, 2011), which equates to wind speeds between 8 and 10.8  
123 m/sec. Intervals of calm are seldom met on this shore. Crossing an enormous fetch, the  
124 trade winds that reach São Nicolau produce ocean swells with wave heights that run  
125 between 3.5 and 6 m (Brand, 2011). The present-day wind field and sea-surface  
126 dynamics make conditions on the windward rocky shore highly energetic. Scouring of  
127 the shore is intense and even small pocket beaches (as at the mouth of Ribeira Alta east  
128 of Juncalinho) are rare along the north coast. The island's largest sand beaches are found  
129 around Tarrafal de São Nicolau on the sheltered, southwest side of the island (Fig. 1).

130

## 131 *2.2. History of volcanism*

132           São Nicolau corresponds to an elongated shield volcano in an early post-erosional  
133 stage of development. The island's geomorphology and structure indicate development  
134 by composite fissure volcanism along two main rift arms. The more prominent is  
135 oriented E–W to WNW–ESE in direction, whereas the lesser is oriented N–S comprising  
136 the western portion of the island (Ramalho et al., 2010a). The island's volcanic history  
137 extends from the Miocene to the Quaternary (Macedo et al., 1988; Duprat et al., 2007;  
138 Ramalho et al., 2010a, b).

139           Emergence of the earliest landmass belonging to present-day São Nicolau  
140 occurred sometime during the Mid- to Late Miocene and corresponds to the Old Eruptive  
141 Complex. This unit, which remains undated, mostly comprises intensely palagonitized  
142 hyaloclastites pervasively intruded by a dyke swarm (Macedo et al., 1988; Ramalho,  
143 2011). Marine sediments and submarine lavas rest unconformably above this unit. The  
144 first corresponds to shallow-water calcarenites (Monte Focinho Formation) with an  
145 estimated age between 11.8 and 5.8 Ma or even between 6.2 and 5.8 Ma (Bernoulli et al.,  
146 2007), whereas the latter corresponds to an entirely submarine volcanic unit (Figueira de  
147 Coxe Formation) that erupted between 6.2 and 5.8 Ma (Duprat et al., 2007; Ramalho et  
148 al., 2010b). The Figueira de Coxe Formation crops out at elevations in excess of 270 m  
149 above sea level attesting to episodic uplift that has affected São Nicolau since its first  
150 emergence (Ramalho et al., 2010a, b, c).

151           After a brief period of volcanic quiescence, uplift, and erosion, during which  
152 coastlines and adjacent shelves matured, the edifice of São Nicolau experienced a period  
153 of renewed and vigorous volcanic activity that corresponds to the Main Eruptive  
154 Complex (Macedo et al., 1988; Ramalho et al., 2010a, b). During this stage, coastlines  
155 rapidly expanded by lateral progradation of effusive lava deltas that covered large swaths  
156 of the pre-existing island shelf and preserved existing shelf sediments within the volcanic  
157 sequence. The main shield-building stage on São Nicolau lasted approximately 2.5  
158 million years, from 5.0 to 2.5 Ma before present (Duprat et al., 2007; Ramalho et al.,  
159 2010b), a period during which coastlines constantly and rapidly shifted as volcanic  
160 activity and erosion counterbalanced each other. Finally, around 2.5 Ma, São Nicolau  
161 entered a period of slow erosional decay, interrupted by two intervals of volcanic

162 rejuvenation that correspond to the Preguiça and Monte Gordo formations, respectively at  
163 1.7–0.7 Ma and <100 ka (Duprat et al., 2007; Ramalho et al., 2010b).

164

### 165 2.3. *Previous paleontological studies*

166 Earlier studies on the paleontology of São Nicolau were conducted by Bebiano  
167 (1932), Torres and Soares (1946), Serralheiro and Ubaldo (1979), and Macedo et al.  
168 (1988). Torres and Soares (1946) identified some species of fossil rhodoliths belonging  
169 to the genus *Lithothamnion*, including material from Monte Focinho. A more recent  
170 study by Bernoulli et al. (2007) provided a reappraisal of the taxonomy and age of key  
171 fossils from the limestone at Monte Focinho near the island's south-central coast (Fig. 1).  
172 A Late Miocene age was established both on the basis of benthic foraminifera in the  
173 genus *Amphistegina* and planktic foraminifera assigned to species of *Globigerina*,  
174 *Globigerinoides*, *Globorotalia*, and other genera. The grainstone from this locality  
175 includes the abundant debris of cirripede barnacles mixed with lesser amounts of  
176 coralline red algae fragments that accumulated below a steep, rocky shore.

177

### 178 **3. Methods**

179 The approximate size and configuration of the island of São Nicolau during the  
180 Late Miocene and immediately prior to the onset of the Main Eruptive stage at ~5.1 Ma  
181 (Ramalho et al., 2010b) was reconstructed using the present outcrop pattern of the Old  
182 Eruptive Complex and Figueira de Coxe Formation in conjunction with relative sea-level  
183 information extracted from the volcanic succession at Castilhano (sometimes written  
184 Castilhiano). In this place, the first erupted lavas of the Main Eruptive Complex (dated at



185 5.09±0.07 Ma) preserved a paleo-coastline that presently can be found at ~100 m of  
186 elevation (Ramalho et al., 2010a,b). Thus, using the Castilhano succession as a pivot  
187 point, the shape and dimensions of proto-São Nicolau were extrapolated around the  
188 perimeter defined by all outcrops of the Old Eruptive Complex and Figueira de Coxe  
189 Formation pene-contemporaneous in position. On the northern coast, where marine  
190 erosion already reduced the island considerably, the approximate position of the 100-m  
191 isobath was used to speculate where the northern limit of the island edifice was located  
192 during the Late Miocene.

193 Strip logs for stratigraphic sections modified after the standard format used by  
194 Shell Oil Company were compiled for four localities divided between the north and south  
195 shores of São Nicolau. In addition to rhodoliths, care was taken to register occurrences  
196 of shelly macrofossils and trace fossils. Samples also were collected for calcareous  
197 nannofossils, generally limited to finer grained and less indurated layers in the carbonate  
198 succession. The fine fractions from samples were concentrated in laboratory test tubes  
199 through overnight settling from a vigorously shaken half-sediment, half-tap-water  
200 suspension. The top fine fraction was extracted directly to a cover glass by a Pasteur  
201 pipette, spread into a rippled smear, and permanently mounted. Smear slides were  
202 scanned for coccoliths on a petrographic microscope (Zeiss Ortholux II-Pol) at x1250  
203 magnification along a 3-cm column (approximately 5 mm<sup>2</sup>). Calcareous nannofossil  
204 taxonomy follows criteria standardized by Perch-Nielsen (1985) and Bown (1998).  
205 Rhodolith samples from two levels at Castilhano were collected for identification at the  
206 genus level using petrographic thin sections.

207 Whole rhodolith specimens from specific stratigraphic intervals were measured  
208 on site (to the nearest millimeter) across three principal axes (long, intermediate, and  
209 short). Data from these measurements were subjected to analysis based on the triangular  
210 plot among spherical, ellipsoidal, and discoidal shapes according to the format applied to  
211 rhodoliths by Bosence (1976, 1983) as modified from Sneed and Folk (1958).

212

## 213 **4. Results**

### 214 *4.1. Island reconstruction for the Late Miocene*

215 Coastline reconstructions for a Late Miocene (5.7–5.1 Ma) island indicate an  
216 elongated edifice approximately 25–33 km in length in an east-west dimension, and at  
217 least 8-10 km of maximum width in the north-south dimension (Fig. 2). The lack of  
218 outcrops of the Old Eruptive Complex and Figueira de Coxe Formation in an area east of  
219 Juncalinho and in the vicinities of Ribeira Alta precludes any more solid reconstructions  
220 for this part of the edifice.

221

### 222 *4.2. North shore stratigraphy and paleontology*

223 Stratigraphic profiles from the oasis at Castilhano and the canyon walls of Ribeira  
224 de Covoada de Bodela (Fig. 3) detail the onlap of carbonate deposits against rocky shores  
225 located on the northeast flank of Miocene São Nicolau (Figs. 1–2). Both sections are  
226 constrained below by the Old Eruptive Complex (intensely altered hyaloclastites and  
227 basaltic lava flows) and above by basaltic lava flows belonging to the onset of the Main  
228 Eruptive Complex. Both sections include abundant rhodoliths and both replicate a  
229 fining-up pattern through the first 3-4 m at which point the Bodela section terminates.

230 Thereafter, the Castilhano section recommences with renewed coarsening and rhythmic  
231 fining and coarsening in thick beds before a final fining-upwards sequence. The lower  
232 part of the carbonate succession at Castilhano is packed with rhodoliths that over-ride an  
233 irregular basalt surface with a topographic relief of about 1 m, including small overhangs  
234 of basalt under which rhodoliths are trapped (Fig. 4A and B). A basalt boulder above the  
235 unconformity exhibits a cluster of circular depressions 4 cm in diameter (Fig. 4C) that  
236 match the typical dwelling structures of regular echinoids assigned to the ichnospecies  
237 *Circolites kotoncensis*. Rhodoliths are less common in the stratigraphic interval between  
238 2.5 m to 4 m above the unconformity, but thereafter resume in abundance (Fig. 3). An  
239 interval directly below the 4-m horizon features the trace fossil *Thalassinoides suevicus*  
240 (Fig. 4D).

241 Many rhodoliths reveal a small rock core of basalt in cross section (Fig. 4E).  
242 Sampled from a horizon 40 cm above the unconformity, the average maximum diameter  
243 of rhodoliths is 3.3 cm. Higher at a level 2.5 m above the unconformity, the average  
244 maximum diameter of rhodoliths registers an increase to 3.75 cm. The rhodoliths from  
245 these two levels are identified as belonging to the genus *Lithothamnion* (Davide Bassi,  
246 personal communication, 2013). Pectinid bivalves and *Spondylus* sp. together with  
247 broken tests of the echinoid *Clypeaster* sp. are more common in the upper half of the  
248 exposure than in the lower half. Loose plates of the cirriped barnacle *Balanus* sp. appear  
249 in the top two meters of the exposure.

250 At half the thickness of the Castilhano section, the Bodela section (Fig. 3) also  
251 exhibits an unconformity surface with about 1 m of relief on submarine basalt but is  
252 notably different in development of a distinct basal conglomerate with eroded clasts up to

253 45 cm in diameter (Fig. 4F). Rhodoliths with an average maximum diameter of 3.5 cm  
254 are plentiful through the overlying section, but not quite as abundant as found in the  
255 Castilhano section. In addition to *Pecten* sp. and *Spondylus* sp., associated bivalves  
256 include oysters encrusted on basalt boulders and the infaunal bivalves *Cardium* sp. and  
257 *Venus* sp. As at Castilhano, broken pieces of tests belonging to *Clypeaster* sp. occur, but  
258 also the spines of a cidaroid echinoid. Barnacles appear in the Bodela section attached  
259 only to bivalves. Rare pieces of the finger coral *Porites* sp. represent a faunal element at  
260 Bodela not observed at Castilhano.

261

#### 262 4.3. Fossil rhodolith shape analyses

263 Although the shallow-water marine assemblages of Castilhano and Bodela are  
264 somewhat diverse, rhodoliths are the dominant element contributing to the limestone.  
265 Samples of whole rhodoliths varying in number from 35–40 specimens were extricated  
266 for measurements from narrowly defined stratigraphic intervals at both localities.  
267 Comparison shows that the most spheroidal rhodoliths come from an interval 40 cm  
268 above the base of the Castilhano section with a spread almost entirely restricted to the  
269 upper triangle in the larger triangular plot (Fig. 5A). Higher in the Castilhano section  
270 (2.5 m above the unconformity), rhodoliths are slightly larger in size and exhibit a slight  
271 tendency to more ellipsoidal shapes indicated by the spill-over of roughly half the sample  
272 into other sectors below and to the right of the upper triangle (Fig. 5B). The rhodolith  
273 sample from the Bodela section (Fig. 5C) comes from a level directly above the basal  
274 conglomerate (Fig. 3). In the range of shapes, it is more like the lower sample from  
275 Castilhano, but with a very few points that spill outside the upper triangle in a pattern

276 similar to the upper sample from Castilhano. The majority of rhodoliths from both  
277 sections is highly uniform in size and shape.

278

279 *4.4. South shore stratigraphy and paleontology*

280 A stratigraphic profile from Baía dos Barreiros (Fig. 6) details the onlap of carbonate  
281 deposits against rocky shores eroded in the Old Eruptive Complex located on the  
282 southeast flank of Miocene São Nicolau (Fig. 2). In this region, the carbonates crop out  
283 near the base of sea cliffs for 2.5 km from Baía dos Barreiros to Ponta Barroso (Fig. 2).  
284 Sediments constitute a 4 to 5 m evenly thick band, dipping about 10° to the south. In  
285 detail, however, the internal structure exhibits prograding foresets dipping about 15–20°  
286 to the south. Sediment composition is overwhelmingly dominated by intermediate-to-  
287 coarse rhodolith debris with very low amounts of lithics. Abraded rhodoliths are present  
288 but extremely rare, as well as other macrofossils. The succession generally exhibits a  
289 fining-up pattern, but terminates with a conglomerate that features pebbles derived from  
290 the Old Eruptive Complex (Fig. 6). Intervals with the trace-fossil *Thalassinoides* isp.  
291 occur at 1.25 m and 3.8 m above the base of the section; the trace-fossils *Sinusichnus* isp.  
292 and ?*Ophiomorpha* isp appear at a horizon 3 m above the base of the section. These  
293 trace-fossils are known to have a wide depth range in littoral to outer shoreface settings  
294 (Mayoral et al., 2013). An erosive unconformity is inferred at the top of the sedimentary  
295 succession, as shown by truncation of a basaltic dyke. The sediments along Baía dos  
296 Barreiros occur at the same stratigraphic position found at Castilhano and Ribeira de  
297 Covoada de Bodela. As such, these sections are considered to be pene-contemporaneous.

298 Extensive sedimentary outcrops on the south shore are exposed through the  
299 canyon of the Ribeira da Ponta da Pataca, located about 800 m south-southwest of the  
300 village of Preguiça (Fig. 1). Stratigraphic profiles for Pataca 1 (Fig. 6) and Pataca 2 (Fig.  
301 7) are laterally continuous over 130 m and represent respective distal and more proximal  
302 settings in relationship to a former paleoshore. The thicker succession at Pataca 1  
303 commences 17 m above present sea level, whereas the thinner succession at Pataca 2  
304 starts at about 60 m above present sea level and follows inland along the narrow  
305 streambed of Ribeira da Ponta da Pataca. Well-defined beds near the top of the  
306 succession dip about 6 to 8° to the southeast. A pile of submarine sheet flows rest  
307 conformably above the fossiliferous sediments. The transition to subaerial flows is  
308 poorly observed as the outcrops are extensively covered by scree.

309 At Pataca 1, the outcrop consists of three coarsening-up intervals with echinoid  
310 tests and spines present throughout. The initial coarsening-up sequence is a massive,  
311 very sandy and poorly sorted limestone or calcareous sandstone (Fig. 8A). Whole  
312 macrofossils are few, but the bivalve *Pinna* sp. is preserved in life position. In addition,  
313 short branching colonies of *Porities* sp. (Fig. 8B) occur together with thin, stick-shaped  
314 bryozoans of *Thalamoporella* sp. (Fig. 8C) that are commonly encrusted by a more  
315 delicate bryozoan attributed to *Metrarabdotos* sp. The trace fossils *Ophiomorpha nodosa*  
316 and *Macaronichnus segregatis* range through most of the initial interval. A second  
317 coarsening-up interval is a more pure limestone with higher fossil content that includes  
318 coral fragments and coquinas of *Argopecten* aff. *flabellum* (Fig. 8D). *Balanus* plates also  
319 are present. Many fossils are encrusted by bryozoans and serpulids. The trace fossil  
320 *Ophiomorpha nodosa* occurs at the very base of the interval, but otherwise trace fossils

321 are absent. A third coarsening-up interval begins with minor basalt clasts and changes to  
322 a well-sorted lithic sandstone with little fossil content. Echinoids are the most common  
323 fossils in this interval, but *Balanus* plates also are present. The trace fossil *Skolithos*  
324 *linearis* (Fig. 8E) dominates the top 60 cm of this interval. The sediments seem to rest  
325 upon volcanoclastic breccia that may correspond to collapsed material and/or deposits of  
326 submarine debris flows.

327         The upper part of Pataca 1 is physically continuous with the lower part of Pataca  
328 2. Being more proximal, however, Pataca 2 differs laterally in exhibiting a much higher  
329 content of basaltic clasts (Fig. 8F). The section shows a change from sandy limestone to  
330 calcareous sandstone (Fig. 7) with increasingly better sorting. The trace fossil  
331 *Thalassinoides suevicus* occurs near the base of the section. The lower layers are very  
332 fossiliferous, changing upwards to more bioclastic content. The gastropods *Strombus* sp.  
333 and *Turritella* sp. together with pectinid bivalves and barnacles are very common. Some  
334 coral colonies of *Tubastrea* sp. with conspicuous borings by pholad bivalves (Fig. 8G)  
335 are encrusted together with serpulids on basalt cobbles. The upper part of this section is  
336 formed by massive sandstone with fewer fossils. Echinoids spines, transported and worn  
337 *Porites* colonies and fragments of *Pecten* shells are present, as well as a sparse  
338 representation of the trace fossil *Ophiomorpha nodosa*.

339

#### 340 4.5. Calcareous nannofossil biostratigraphy

341         Samples for age-diagnostic nannofossils were collected at three levels through the  
342 stratigraphic succession at Castilhano (see Fig. 3) both with and without rhodoliths.  
343 Species common to all three samples include *Dictyococcites antarcticus*, *D. productus*,

344 *Reticulofenestra haqii-minutula*, and *R. pseudoumbilicus*. The abundance of calcareous  
345 nannofossils showed an increase up-section, consistent with the transgressive nature of  
346 the succession. No species were exclusive to the horizon rich in rhodoliths. Species  
347 common to the upper samples but lacking from the lowest sample include *Calcidiscus*  
348 *leptoporus*, *Ciclicargolithus floridanus*, *Discaster* sp., small *Reticulofenestra* sp., *R.*  
349 *rotaria*, *Sphenolithus abies*, and *Syracosphaera* sp. The assemblage is compatible with a  
350 Late Miocene (Messinian) age (Bown, 1998). Notably, *R. rotaria* has a known First  
351 Appearance Datum (FAD) of 7.42 Ma and Last Appearance Datum (LAD) of 6.91 Ma.

352 A single sample was collected from the up-stream section at Ribeira Covoada de  
353 Bodela (see Fig. 3). The diversity of calcareous nannofossils is lower than that found at  
354 any level at Castilhana, but includes many of the same species indicative of correlation  
355 with the Messinian Stage.

356 Samples were collected at three levels through the Pataca 1 section (see Fig. 7).  
357 The sample from the lower layers is low in diversity with only three species:  
358 *Braarudosphaera* cf. *rosa*, *Coronocyclus nitescens*, and *Discoaster* sp. The sample from  
359 the middle layers proved to be barren of nannofossils. Finally, a sample from the upper  
360 layers yielded an assemblage including *Calcidiscus leptoporus*, *Coccolithus pelagicus*,  
361 *Helicosphaera carteri*, *Reticulofenestra productus*, *R. minuta*, *R. haqii-minutula*, *R.*  
362 *antarticus*, *R. pseudoumbilicus*, *Pontosphaera* sp. and *Umbilicosphaera* sp. This  
363 assemblage is compatible with a Pliocene position due to the presence of several  
364 reticulofenestrids, including *R. pseudoumbilicus* (Bown, 1998).

365

366 4.6. Summary of dichotomous biofacies



367 Using biofacies from the northerly Upper Miocene deposits at Castilhana and  
368 Bodela (Fig. 3), it is instructive to draw contrasts with the southerly pene-  
369 contemporaneous deposits from Baía dos Barreiros (Fig. 6), augmented by data collected  
370 by Bernoulli et al. (2007) from the south-central coast of São Nicolau. All four  
371 successions are seated on the Old Eruptive Complex as defined by Macedo et al. (1988).  
372 Loose barnacle plates are present at the Monte Focinho and Castilhana localities, as well  
373 as whole barnacles attached to shells at Bodela, indicating an initially shallow-water  
374 source for the deposits. Likewise, dwelling structures eroded by regular echinoids in a  
375 basalt boulder at Castilhana (Fig. 4C) confirm such a relationship. In addition to the  
376 various benthic and planktic foraminifera recovered from the Monte Focinho section,  
377 Bernoulli et al. (2007) described a bioclastic grainstone that incorporates echinoid spines  
378 and bits of red algae, although the limestone's dominant signature comes from barnacle  
379 debris. No traces of whole or fragmentary rhodoliths were detected during our visit to the  
380 Monte Focinho locality.

381 Further comparisons may be drawn between the Miocene sequence at Castilhana  
382 and the Pliocene sequence at Pataca. The former registers two deepening phases of  
383 deposition on an open marine sublittoral platform signified by rhythmic fining-upward  
384 beds in the middle of the succession (Fig. 3). In contrast, the Pataca 1 section records  
385 three coarsening-upward phases with considerably greater content of terrestrial lithics  
386 (Fig. 6). Of these, only the two upper sequences shallow sufficiently to reach relatively  
387 high-energy conditions. The presence of both whole and crushed valves belonging to  
388 pectinid bivalves indicates landward transport from an open, offshore area to the south,  
389 whereas barnacles record input from a closer, near-shore zone. This overall scenario has

390 implications for the development of a distal delta on the leeward side of São Nicolau.  
391 The most striking omission from this Pliocene scenario is the complete lack of rhodoliths  
392 or rhodolith debris. This is in marked contrast to the older Castilhano and Bodela  
393 sections on the windward side of São Nicolau, where rhodoliths (Fig. 4F) constitute the  
394 primary carbonate signature showing shoreward transport against rocky shores. For the  
395 most part, these deposits signify death assemblages, because photosynthesis by the  
396 coralline red algae ceased for all but the top layer of rhodoliths in the transported  
397 package.

398

## 399 **5. Discussion**

### 400 *5.1. Reconfiguration of a Miocene island*

401 The coastline reconstructions for a Late Miocene island (Fig. 2) portray a smaller  
402 edifice than the present-day São Nicolau. This is not surprising, as these reconstructions  
403 correspond to a moment in time that immediately preceded the onset of the main shield  
404 building stage, during which the island grew considerably in size. Notwithstanding its  
405 smaller size, São Nicolau already constituted a prominent east-west elongated volcanic  
406 edifice that extended from 25 to 33 km in length during the Late Miocene. This volcanic  
407 edifice essentially emerged above the sea surface by means of uplift and not summit  
408 volcanism, as attested to by onlap of a dominantly subaerial Main Eruptive Complex over  
409 the eroded remains of an entirely submarine edifice corresponding to the Old Eruptive  
410 Complex and Figueira de Coxe Formation.

411

### 412 *5.2. Composition and morphodynamics of São Nicolau rhodoliths*

413           The Upper Miocene rhodoliths from the northern shores of São Nicolau are  
414 characterized by three key traits. They are comparatively small, exceedingly well  
415 rounded, and are represented by the single genus *Lithothamnion*. As demonstrated  
416 through shape analyses (Fig. 5), these rhodoliths are among the most spherical detected  
417 so far in studies on living and fossil rhodoliths from the Cape Verde and Canary islands  
418 (Johnson et al., 2012). Practically, such shapes make good rollers that are susceptible to  
419 transport; therefore it is not surprising to find thick rhodolith accumulations on the  
420 windward side of paleoislands. According to Braga et al. (2010), the taxonomic  
421 composition of Miocene coralline assemblages and growth forms changes with depth that  
422 parallels present-day conditions. For example, the mastophoroid and lithophylloid  
423 rhodoliths are typical of shallower-water settings, whereas the melobesioids (which  
424 include *Lithothamnion*) tend to represent deeper-water settings. On this basis, it may be  
425 argued that the São Nicolau rhodoliths that typically nucleate around small basalt cores  
426 were transported shoreward from deeper waters.

427           The sedimentological signature imparted by rhodoliths on the paleoshores of  
428 Miocene São Nicolau are strongly related to physical transportation. On the northeast  
429 shore at Castilhano and Bodela (Fig. 3), relatively small rhodoliths were left intact but  
430 rolled shoreward by the action of strong surf to abut directly against rocky shores. In  
431 some cases, the rhodoliths fill spaces below bedrock overhangs. In contrast, the fact that  
432 only rhodolith debris is present on the leeward southern shores at Ponta Barroso and Baía  
433 dos Barreiros (Figs. 2 and 6) indicates that long-shore currents and wave refraction was  
434 the dominant influence in transporting materials to the southern shelf. The internal

435 structure of these beds with distinct foresets suggests that sediments were deposited as  
436 clinoforms directed offshore to the south.

437

### 438 5.3. Comparison with other windward-leeward systems

439 Examples from the literature (e.g. Johnson, 2002; Johnson and Baarli, 2012)  
440 typically relate to former islands on flooded continental shelves. The only case of a  
441 windward and leeward system previously studied from a fully oceanic setting on a basalt  
442 island comes from Porto Santo in the Madeira archipelago. At the Cabeço das Laranjas  
443 on the windward side of Ilhéu de Cima off Porto Santo, thick Middle Miocene deposits of  
444 large rhodoliths represented by the genera *Lithothamnion*, *Sporolithon*, and  
445 *Neogoniolithon* are impounded against the original basalt shore (Johnson et al., 2011).  
446 As in the Castilhano and Bodela sections on São Nicolau, rhodoliths in such transported  
447 deposits were deprived of sunlight and soon perished. In contrast, the leeward shore of  
448 Ilhéu de Cima at Pedra de Água features a coeval Middle Miocene setting with coral  
449 colonies fixed in growth position on basalt mounds that rise above a sandy zone over  
450 which no more than one or two layers of rhodoliths are emplaced (Santos et al., 2012,  
451 their figs. 1 and 9). Nearly all the rhodoliths observed in cross-section at Pedra de Água  
452 are nucleated around large basalt pebbles, whereas many of the rhodoliths at the Cabeço  
453 das Laranjas lack a rock core. The rhodoliths at Pedra de Água are polyspecific from the  
454 genera *Lithophyllum* and *Sporolithon* and considered to have grown in shallow, subtidal  
455 waters close to the paleoshore (Santos et al., 2012), whereas those at the Cabeço das  
456 Laranjas were swept towards land from deeper waters by major storms of hurricane  
457 strength (Johnson et al., 2011).

458

459 *5.3. Shifting Miocene wind and storm patterns*

460           Based on stratigraphic data regarding variations in marine benthic  $\delta^{18}\text{O}$  isotopes,  
461 related models for reconstruction of mean sea-surface temperatures, and sea-level  
462 variations pegged to ice-sheet models cited by De Boer et al. (2012, their fig. 1), the  
463 Middle Miocene Climatic Optimum (MMCO) stands out among major climatic shifts  
464 during the last 34 million years. Termination of this phase coincides with expansion of  
465 the East Antarctic Ice Sheet corresponding to distinct pulses dated to 13.8 and 13.2 Ma  
466 (Westerhold et al., 2005). Global temperatures not only began to receded with the  
467 decline of the MMCO, but evidence from places as distant as the South China Sea and  
468 the Mediterranean Sea suggests that the Intertropical Convergence Zone (ITCZ) was  
469 pushed substantially northward from a position near the equator (John et al., 2003;  
470 Holbourn et al., 2010).

471           A displaced ITCZ could be expected to have a profound effect on climate in the  
472 developing Macaronesian archipelagos of the eastern North Atlantic, including the Cape  
473 Verde islands. In place of steady trade winds that normally arrive from the northeast, the  
474 flow of winds would shift to blow from the southeast. More typical of trade winds in the  
475 Southern Hemisphere, these would brush locally parallel to the West African coast and be  
476 more likely to stimulate sustained marine upwelling. More significant, the northward  
477 migration of the ITCZ should alter the general staging area and subsequent storm tracks  
478 of hurricanes in the North Atlantic. This scenario was employed to account for the  
479 occurrence of major storm deposits formed by Middle Miocene rhodoliths at Cabeço das

480 Laranjas on Ilhéu de Cima off Porto Santo in the Madeira archipelago (Johnson et al.,  
481 2011).

482 Emerging Northern Hemisphere glaciations that intensified through post-Miocene  
483 times served to re-balance the ITCZ and facilitate its return to regions around the equator.  
484 A stable isotope study based on stratigraphy from the southeastern Atlantic (Vidal et al.,  
485 2002) shows a rapid decrease in  $\delta^{18}\text{O}$  values consistent with a general warming trend in  
486 that part of the world already by Messinian time during the Late Miocene. Such a result  
487 suggests that a scenario similar to pattern of strong northeasterly trade winds across the  
488 Maraconesian realm, including the Cape Verde archipelago, was in effect by the end of  
489 the Miocene. Hence, present-day climate patterns dominated by persistent trade winds  
490 from the northeast against the island of São Nicolau (Brand, 2011) should serve as a  
491 reliable guide for comparison of windward and leeward coastal deposits of Late Miocene  
492 and Pliocene age around the island.

493

#### 494 *5.4. Use of volcanic sequences to gauge absolute water depth*

495 Effusive coastal volcanic successions such as those resulting from the extrusion of  
496 lava-fed deltas provide additional constraints on coeval sea level and consequently on  
497 paleo-water depths of bottomset sediments (Porebski and Gradzinski, 1990; Ramalho,  
498 2011; Johnson et al., 2012; Meireles et al., 2013). During low- to moderate- effusion rates  
499 (Ramalho et al., 2013), lava flows entering the sea typically form structures similar to  
500 Gilbert-type deltas, with foresets of pillow lavas and hyaloclastites overlain by a topset of  
501 subaerial lavas; the passage zone between these two components of the delta thus marks  
502 very accurately contemporaneous sea level (Porebski & Gradzinski, 1990; Ramalho,

503 2011). The vertical distance between the sedimentary bottomset (typically corresponding  
504 to marine sediments coeval of the eruption) and the passage zone, along the dip of the  
505 foresets, is thus a reliable way of estimating the palaeo-water depth of the sediments  
506 (Ramalho, 2011; Johnson et al., 2012; Meireles et al., 2013).

507 At Castilhano (Fig. 3), a typical lava-delta succession with foresets of pillow lavas  
508 and hyaloclastites overly the marine sediments and the passage zone between overlying  
509 submarine and subaerial basalt occurs 25 m above the top of the limestone, pinpointing  
510 coeval stage of sea level around 5.09 Ma (Ramalho et al., 2010b). At Bodela (Fig. 3), the  
511 sedimentary sequence is overlain by massive submarine flows, and the passage zone  
512 between overlying submarine and subaerial basalt occurs 35 m above the top of the  
513 limestone in the Bodela section, suggesting a slightly deeper deposition than at  
514 Castilhano. Farther south at Baía dos Barreiros, the passage zone is 95 m above the  
515 Upper Miocene limestone (Ramalho et al., 2010a), marking the terminal depth of that  
516 limestone as much deeper. At this locality, however, the value should be treated with  
517 caution, because an unconformity marked by a truncated dike occurs between the  
518 sediments and overlying lava flows. For these three localities, the passage zone between  
519 subaerial and submarine lava flows is coeval and signifies the same relative sea level now  
520 marked 100 m above the present. Measurements of accommodated water depth at the  
521 time carbonate deposition ceased at Castilhano, Bodela, and Baía dos Barreiros in the  
522 Late Miocene agree reasonably well with fossil content.

523 At Ribeira da Ponta da Pataca on the south-central coast, the observable passage  
524 zone in volcanics overlying Pliocene sedimentary strata is approximately 90 m above  
525 present-day sea level, indicating a possible coeval water column of 35 to 40 m for Pataca

526 2 (Fig. 7) and 60 to 70 m for Pataca 1 (Fig. 6). The difference in paleo-water depth at  
527 these two localities is an artifact of the natural slope on the Pliocene sea floor. Because  
528 the capping volcanic sequence shared by the two sections consists of a pile of low-angle  
529 submarine sheet flows, there may have been a time lapse between the moment of burial  
530 and the transition to subaerial flows at the passage zone above. Other possible  
531 disconformities may be hidden in the covered interval between the sedimentary strata and  
532 subaerial basalt. A hiatus of any duration may mask an intermittent rise in sea level. In  
533 any case, the *Skolithos* trace fossils at the top of Pataca 1 (Fig. 6) typically reflect a water  
534 depth shallower than suggested by the overlying passage zone. At Portinho da Mulher  
535 Branca near Praia on Santiago island, for example, *Skolithos* was related to an overlying  
536 passage zone indicating a water depth of only 12 to 15 m (Johnson et al., 2012). This  
537 discrepancy in conflicting water-depth indicators remains to be resolved either by  
538 extending the bathymetric range of the ichnofossil or by an obfuscating time gap.

539

## 540 **6. Conclusions**

541 Examples of contrasting windward and leeward settings from paleoislands are  
542 well documented, but mainly from continental shelves. The distribution and fossil  
543 content of surviving Upper Miocene limestone strata on São Nicolau are limited but  
544 adequate to outline patterns in intertidal to shallow, sub-tidal biofacies in close proximity  
545 to rocky shores influenced by winds and waves around one of the windward volcanic  
546 islands in the Cape Verde Archipelago. Supplementary data from a comparatively thick  
547 Pliocene succession on the island's south-central shore provide further insight on the



548 potential richness achieved by biofacies in a setting better sheltered from wave shock.

549 Four core conclusions highlight the results of this study.

550 1. Limestone dominated by whole rhodoliths follows a distinct band correlated from  
551 the oasis at Castilhano to the canyon of the Ribeira de Covoada de Bodela on the  
552 northeast flank of São Nicolau. Relatively small in size, the rhodoliths were  
553 swept shoreward from a shallow bank situated nearby to the north or northeast.  
554 Many are nucleated around basalt pebbles eroded from an adjacent rocky shore.  
555 These algal concretions accumulated in vast numbers as a transported assemblage  
556 deposited against the rocky shore, even pressed to fill spaces below overhangs in  
557 the bedrock. Although poor in calcareous nannofossils, the identified assemblage  
558 is compatible with a Late Miocene (Messinian) assignment.

559 2. Whole rhodoliths are absent from the coeval limestone at Baía dos Barreiros in  
560 southeast São Nicolau but extensive rhodolith sand is well developed as clinoform  
561 structures dipping seaward to the south. The more loosely equivalent limestone at  
562 Monte Focinho near the island's south-central shore also includes fine debris of  
563 coralline red algae mixed with crushed barnacles. A more sandy limestone  
564 deposit of Pliocene age at Ribeira da Ponta da Pataca on the south-central coast  
565 includes elements such as the whole (and broken) valves of pectinid bivalves, as  
566 well as whole branches of the *Porites* coral and delicate *Thalamoporella* bryozoa  
567 that are unusual or entirely absent from deposits on the north side of the island. A  
568 Pliocene age for the Pataca deposits based on calcareous nannofossils concurs  
569 with the age of basaltic lavas near the overlying passage zone dated at  $3.06 \pm 0.17$   
570 Ma.

571 3. With a change after the Middle Miocene Climatic Optimum that brought the  
572 Intertropical Convergence Zone closer to the equator, the Late Miocene and  
573 Pliocene conditions at São Nicolau experienced steady winds from the northeast  
574 that generated ocean swell. Although smaller than today by perhaps 40%, the  
575 Late Miocene island still presented a long east-west oriented northern shore that  
576 felt the full impact of these conditions, much as today. Thus, the fossil deposits at  
577 Castilhano and Bodela represent accumulations on an exposed, windward coast,  
578 while those at Baía dos Barreiros and Pataca are indicative of a more sheltered,  
579 leeward coast.

580 4. Upper Miocene limestone beds near the northeastern coast at Castilhano and  
581 Bodela are overlain by submarine flows with passage zones to subaerial flows at  
582 intervals 25 m and 35 m above, respectively. Marine onlap of the carbonates  
583 concluded at those water depths with no discrepancy indicated by fossil content.  
584 Certain discrepancies with unconformities and trace fossils remain to be solved,  
585 as in the southern successions. Overall, however, the application of such  
586 transitions in volcanic flows to measure original water depth is a useful technique  
587 in the reconstruction of coastal conditions.

588

#### 589 **Acknowledgments**

590 This study was funded under grant CGL2010-15372-BTE from the Spanish  
591 Ministry of Science and Innovation to project leader Eduardo Mayoral (University of  
592 Huelva). Support from Research Group RNM276 also is acknowledged. Extra support  
593 for work on calcareous nannofossils came from PTDC/MAR/102800/2008. R. Ramalho

594 was funded by an FP7-PEOPLE-2011-IOF Marie Curie Postdoctoral Fellowship, which  
595 is gratefully acknowledged. We thank Dr. Björn Berning (Upper Austrian State  
596 Museum, Leonding, Austria) for identification of the Pataca bryozonas to genus level and  
597 Dr. Davide Bassi (Department of Earth Sciences, Ferrara University, Italy) for  
598 identification of the Castilhano rhodoliths to genus level. The editor and two anonymous  
599 reviewers provided useful comments that helped to improve the final manuscript.

600

## 601 **References**

- 602 Ávila, S., Ramalho, R.S., Vullo, R., 2012. Systematics, palaeoecology and palaeo-  
603 biogeography of the neogene fossil sharks from the Azores (Northeast Atlantic).  
604 *Annales de Paléontologie* 98, 167–189.
- 605 Amen, R.G., Neto, A.I, Azevedo, J.M.N., 2005. Coralline-algal framework in the  
606 Quaternary of Prainha (Santa Maria Island, Azores). *Revista Española de*  
607 *Micropaleontologia* 37, 63–70.
- 608 Baarli, B.G., Cachão, M., Silva, C.M. da, Johnson, M.E., Mayoral, E.J., Santos, A., 2013.  
609 A Middle Miocene carbonate embankment on an active volcanic slope: Ilhéu de  
610 Baixo, Madeira Archipelago, Eastern Atlantic. *Geological Journal*, in press DOI:  
611 10.1002/gj.2513.
- 612 Bebiano, J., 1932. A geologia do Arquipélago de Cabo Verde. *Comunicações dos*  
613 *Serviços Geológicos de Portugal* 18, 167–187.
- 614 Bernoulli, D., Hottinger, L., Spezzaferri, S., Stille, P. 2007. Miocene shallow-water  
615 limestone from São Nicolau (Cabo Verde): Caribbean-type benthic fauna and time  
616 constraints for volcanism. *Swiss Journal of Geosciences* 100, 215–225.

617 Braga, J.C., Bassi, D., Piller, W.E., 2010. Palaeoenvironmental significance of  
618 Oligocene-Miocene coralline red algae - a review. In Mutti, M, Piller, W.E.,  
619 Betzler, C. (eds.), Carbonate Systems During the Oligocene-Miocene Climatic  
620 Transition. International Association of Sedimentologists, Spec. Publ., 42, 165–182.

621 Bosence, D., 1976. Ecological studies on two unattached coralline algae from western  
622 Ireland. *Palaeontology* 19, 71–88.

623 Bosence, D.K.J., 1983. The occurrence and ecology of Recent rhodoliths -a review. In:  
624 Peryt, T.M. (Ed.), *Coated Grains*. Springer-Verlag, Berlin, pp. 217–224.

625 Bown, P., 1998. *Calcareous Nannofossil Biostratigraphy*. Chapman and Hall, Dordrecht,  
626 The Netherlands, 314 p.

627 Brand, S. (Editor), *African severe weather port guide from Naval Research Laboratory in*  
628 *Monterey, California*, last modified April 2011.  
629 [http://www.nrlmry.navy.mil/port\\_studies/africaports/Mindelo/index.html](http://www.nrlmry.navy.mil/port_studies/africaports/Mindelo/index.html);

630 De Boer, B., Van de Wal, R.S.W., Lourens, L.J., Bintanja, R., 2012. Transient nature of  
631 the Earth's climate and the implications for the interpretation of benthic  $\delta^{18}\text{O}$   
632 records. *Palaeogeography, Palaeoclimatology, Palaeoecology* 335–336, 4–11.

633 Dollar, S.J., Tribble, G.W., 1993. Recurrent storm disturbance and recovery: a long-term  
634 study of coral communities in Hawaii. *Coral Reefs* 12, 223–233.

635 Dott, R.H., Jr. 1974. Cambrian tropical storm waves in Wisconsin. *Geology* 2, 243–  
636 246.

637 Duprat, H.I., Friss, J., Holm, P.M., Grandvoinet, T., Sørensen, R.V. 2007. The volcanic  
638 and geochemical development of São Nicolau, Cape Verde Islands: Constraints

639 from field and  $^{40}\text{Ar}/^{39}\text{Ar}$  evidence. *Journal of Volcanology and Geothermal*  
640 *Research* 162, 1–19.

641 Halfar, J., Mutti, M., 2005. Global dominance of coralline red-algal facies: A response to  
642 Miocene oceanographic events. *Geology* 33, 481–484.

643 Holbourn, A., Kuhnt, W., Regenberg, M., Schulz, M., Mix, A., Andersen, N., 2010. Does  
644 Antarctic glaciation force migration of the tropical rain belt? *Geology* 38, 783–786.

645 John, C.M., Mutti, M., Adatte, T., 2003. Mixed carbonate-siliciclastic record on the  
646 North African margin (Malta) – coupling of weathering processes and mid Miocene  
647 climate. *Geological Society of America Bulletin* 115, 217–229.

648 Johnson, M.E., 2002. Paleoislands in the stream: paleogeography and expected  
649 circulation patterns. In: Monegatti, P. Cecca, F. and Raffi, S. (eds.): *International*  
650 *Conference “Paleobiogeography & Paleoecology 2001”*, Piacenza and Castell’  
651 *Arquato 2001. Geobios*, v. 35 (Mémorie Spécial No. 24), pp. 96-106.

652 Johnson, M.E., Baarli, B.G., 2012. Development of intertidal biotas through Phanerozoic  
653 time. In: Talent, J.A. (ed), , *Earth and Life, International Year of Planet Earth*,  
654 *Springer Science+Busines Media B.V.*, pp. 63–128.

655 Johnson, M.E., Baarli, B.C., Cachão, M., Silva, C.M. da, Ledesma-Vázquez, J., Mayoral,  
656 E.J., Ramalho, R.S., Santos, A., 2012. Rhodoliths, uniformitarianism, and Darwin:  
657 Pleistocene and Recent carbonate deposits in the Cape Verde and Canary  
658 archipelagos. *Palaeogeography, Palaeoclimatology, Palaeoecology* 329–330, 83–  
659 100.

660 Johnson, M.E., Silva, C.M. da, Santos, A., Baarli, B.G., Cachão, M., Mayoral, E.J.,  
661 Rebelo, A.C., Ledesma-Vázques, J., 2011. Rhodolith transport and immobilization

662 on a volcanically active rocky shore: Middle Miocene at Cabeço das Laranjas on  
663 Ilhéu de Cima (Madeira Archipelago, Portugal). *Palaeogeography,*  
664 *Palaeoclimatology, Palaeoecology* 300, 113–127.

665 Littler, M.M., Littler, D.S., Murray, S.N., Seaph R.R., 1991. Southern California rocky  
666 intertidal ecosystems. In: Matheison, A.C., Nienhuis, P.H. (eds.), *Intertidal and*  
667 *Litoral Ecosystems. Ecosystems of the World* 24, Elsevier, Amsterdam, pp. 273–  
668 296.

669 MacArthur, R.H., 1972. *Geographical Ecology*. Harper and Row, Publishers, New York,  
670 269 pp.

671 Macedo, J.R., Serralheiro, A., Silva, L.C., 1988. Notícia explicativa da carta da ilha de S.  
672 Nicolau (Cabo Verde) na escala de 1:50 000. *Garcia de Orta, Série Geologia* 11, 1–  
673 32.

674 Mayoral, E., Ledesma-Vázquez, J., Baarli, B.G., Santos, A., Ramalho, R., Cachão, M.,  
675 Silva, C.M. da, Johnson, M.E., 2013. Ichnology in ocean islands; case studies from  
676 the Cape Verde Archipelago. *Palaeogeography, Palaeoclimatology, Palaeoecology*  
677 381–382, 47–66.

678 McNutt, M., 1988. Thermal and mechanical properties of the Cape Verde Rise. *Journal of*  
679 *Geophysical Research (Solid Earth)* 93(B4), 2784–2794.

680 Meireles, R.P., Quartau, R., Ramalho, R.S., Rebelo, A.C., Madeira, J., Zanon, V., Ávila,  
681 S.P., 2013. Depositional processes on oceanic island shelves—evidence from storm-  
682 generated Neogene deposits from the mid-North Atlantic. *Sedimentology* 60, 1769–  
683 1785.

684 Menard, H.W., 1986. *Islands*. Scientific American Library, New York, 219 p.

685 Mitchell-Thomé, R.C., 1972. Outline of the geology of the Cape Verde Archipelago.  
686 Geologische Rundschau 61, 1087–1109.

687 Perch-Nielsen, K., 1985. Cenozoic calcareous nannofossils. In: Bolli, H.H., Saunders,  
688 J.B., Perch-Nielsen, K. (eds.), Plankton Stratigraphy, Volume 1 (2nd edition),  
689 Cambridge Earth Science Series, pp. 329–554.

690 Porebski, S., Gradzinski, R., 1990. Lava-fed Gilbert-type delta in the Polonez Cove  
691 Formation (Lower Oligocene), King George Island, West Antarctica. In: Colella, A.  
692 and Prior, D. (eds), Coarse Grained Deltas, International Association of  
693 Sedimentologists Special Publication 10, 335–351.

694 Ramalho, R.S. 2011. Building the Cape Verde Islands. Springer, 1st Edition, 207 p.

695 Ramalho, R.S., Quartau, R., Trenhaile, A.S., Mitchell, N.C., Woodroffe, C.D., Ávila,  
696 S.P., 2013. Coastal evolution on volcanic oceanic islands: a complex interplay  
697 between volcanism, erosion, sedimentation, sea level change and biogenic  
698 production. Earth Science Reviews 127, 140–170.

699 Ramalho, R.S., Helffrich, G., Vance, D., Schmidt, D.N., 2010a. Tracers of uplift and  
700 subsidence in the Cape Verde Archipelago. Journal of the Geological Society 167,  
701 519–538.

702 Ramalho, R.S., Helffrich, G., Cosca, M., Vance, D., Hofmann, D., Schmidt, D.N., 2010b.  
703 Vertical movements of ocean island volcanoes: Insights from a stationary plate  
704 environment. Marine Geology 275, 84–95.

705 Ramalho, R.S., Helffrich, G., Cosca, M., Vance, D., Hofmann, D., Schmidt, D.N., 2010c.  
706 Episodic swell growth inferred from variable uplift of the Cape Verde hotspot  
707 islands. Nature Geoscience 3(11), 774–777.

- 708 Robertson, A.H.F., 1984. Mesozoic deep-water and Tertiary volcanoclastic deposition of  
709 Maio, Cape Verde Islands: Implications for Atlantic paleoenvironments and ocean  
710 island volcanism. *Geological Society of America Bulletin* 94, 433–453.
- 711 Santos, E., Mayoral, E.J., Silva, C.M. da, Cachão, M., Johnson, M.E., Baarli, B.G., 2011.  
712 Miocene intertidal zonation on a volcanically active shoreline: Porto Santo in the  
713 Madeira Archipelago, Portugal. *Lethaia* 44, 26–32.
- 714 Santos, A.G., Mayoral, E., Johnson, M.E., Baarli, B.G., Silva, C.M. da, Cachão, M.,  
715 Ledesma-Vázquez, J., 2012. Basalt mounds and adjacent depressions attract  
716 contrasting biofacies on a volcanically active Middle Miocene shoreline (Porto  
717 Santo, Madeira Archipelago, Portugal). *Facies* 58, 573–585.
- 718 Serralheiro, A., Ubaldo, M., 1979. Estudo estratigráfico dos sedimentos do Campo da  
719 Preguiça ilha de S. Nicolau (Cabo Verde). *Garcia de Orta, Série Geologia* 3(1-2),  
720 75–82.
- 721 Sneed, E.D., Folk, R.L., 1958. Pebbles in the lower Colorado River, Texas, a study in  
722 particle morphogenesis. *Journal of Geology* 66, 114–150.
- 723 Steiner, C., Hobson, A., Favre, P., Stampfli, G.M., Hernandez, J., 1998. Mesozoic  
724 sequence of Fuerteventura (Canary Islands): Witness of early Jurassic sea-floor  
725 spreading in the central Atlantic. *Geological Society of America Bulletin* 110,  
726 1304–1317.
- 727 Torres, A., Soares, J., 1946. *Formações Sedimentares do Arquipélago de Cabo Verde. I -*  
728 *Actualização de conhecimentos. Junta das Missões Geográficas e de Investigações*  
729 *Coloniais*, 398 p.
- 730 Vidal, L., Bickert, T., Wefer, G., and Röhl, U., 2002. Late Miocene stable isotope



731 stratigraphy of SE Atlantic ODP Site 1085: Relation to Messinian events. *Marine*  
732 *Geology* 180, 71–85.

733 Westerhold, T., Bickert, T., Röhl, U., 2005. Middle to late Miocene oxygen isotope  
734 stratigraphy of ODP site 1085 (SE Atlantic): new constrains on Miocene climate  
735 variability and sea-level fluctuations. *Palaeogeography, Palaeoclimatology,*  
736 *Palaeoecology* 217, 205–222.

737 Zazo, C., Goy, J.L., Hillaire-Marcel, C., Gillot, P.Y., Soler, V., González, J.H., Dabrio,  
738 C.J., Ghaleb, B., 2002. Raised marine sequences of Lanzarote and Fuerteventura  
739 revisited – a reappraisal of relative sea-level changes and vertical movements in the  
740 eastern Canary Islands during the Quaternary. *Quaternary Science Reviews* 21,  
741 2019–2046.

742

### 743 **Figure Captions**

744 **Fig. 1.** Maps at various scales for the North Atlantic archipelagos of Macaronesia with  
745 details shown for the Cape Verde archipelago and the island of São Nicolau.

746 **Fig. 2.** Reconstruction of São Nicolau during the Late Miocene at ~5.1 Ma.

747 **Fig. 3.** Stratigraphic profiles for localities at Castilhano and Ribeira de Covoada de  
748 Bodela on the northeast flank of Miocene São Nicolau.

749 **Fig. 4.** Upper Miocene deposits against basalt unconformities from the northeast part of  
750 São Nicolau showing details of faunal components: A) Irregular unconformity surface  
751 overlain by abundant rhodoliths at Castilhano (figure at right for scale), B) Small  
752 overhang of basalt filled with rhodolith limestone, C) Part of a basalt boulder above the  
753 unconformity surface with dwelling structures formed by regular echinoids assigned to

754 the trace fossil *Circolites kotoncensis*, D) Trace fossil *Thalassinoides suevicus* from mid-  
755 section at Castilhano (see Fig. 3), E) Typical interval packed with rhodoliths many of  
756 which formed around basalt pebbles (arrows), and F) Basal conglomerate and overlying  
757 rhodolith limestone at Ribeira de Covoada de Bodela (figure at left for scale).

758 **Fig. 5.** Triangular plots showing the relative shapes of fossil rhodoliths: A, from the  
759 lower part of the section at Castilhano, B) from the middle part of the section at  
760 Castilhano, and C) from the lower part of the section at Bodela.

761 **Fig. 6.** Stratigraphic profile for the sequence at Baía dos Barreiros on the southeast flank  
762 of Miocene São Nicolau.

763 **Fig. 7.** Stratigraphic profile for the Pliocene coastal sequence at Ribeira da Ponta Pataca  
764 on the southwest flank of Miocene São Nicolau.

765 **Fig. 8.** Stratigraphic profile for the more inland Pliocene sequence at Pataca 2.

766 **Fig. 9.** Pliocene deposits capped by basalt from the southwest coast of São Nicolau at  
767 Ribeira da Pataca: A) Outcrop overview of Pataca 1 (see Fig. 7), B) Cluster of the coral  
768 *Porites* sp. from the lower beds, C) Ramose bryozoan *Thalamoporella* sp. from the lower  
769 beds, D) Disarticulated shells, mostly *Argopecten* aff. *flabellum* from the upper beds, E)  
770 Trace fossil *Skolithos linearis* from the top of the section, F) Outcrop overview of the  
771 Pataca 2 section (see Fig. 8), and G) Coral colonies of *Tubastrea* sp. bored by pholad  
772 bivalves from the middle of the section.

Figure 1

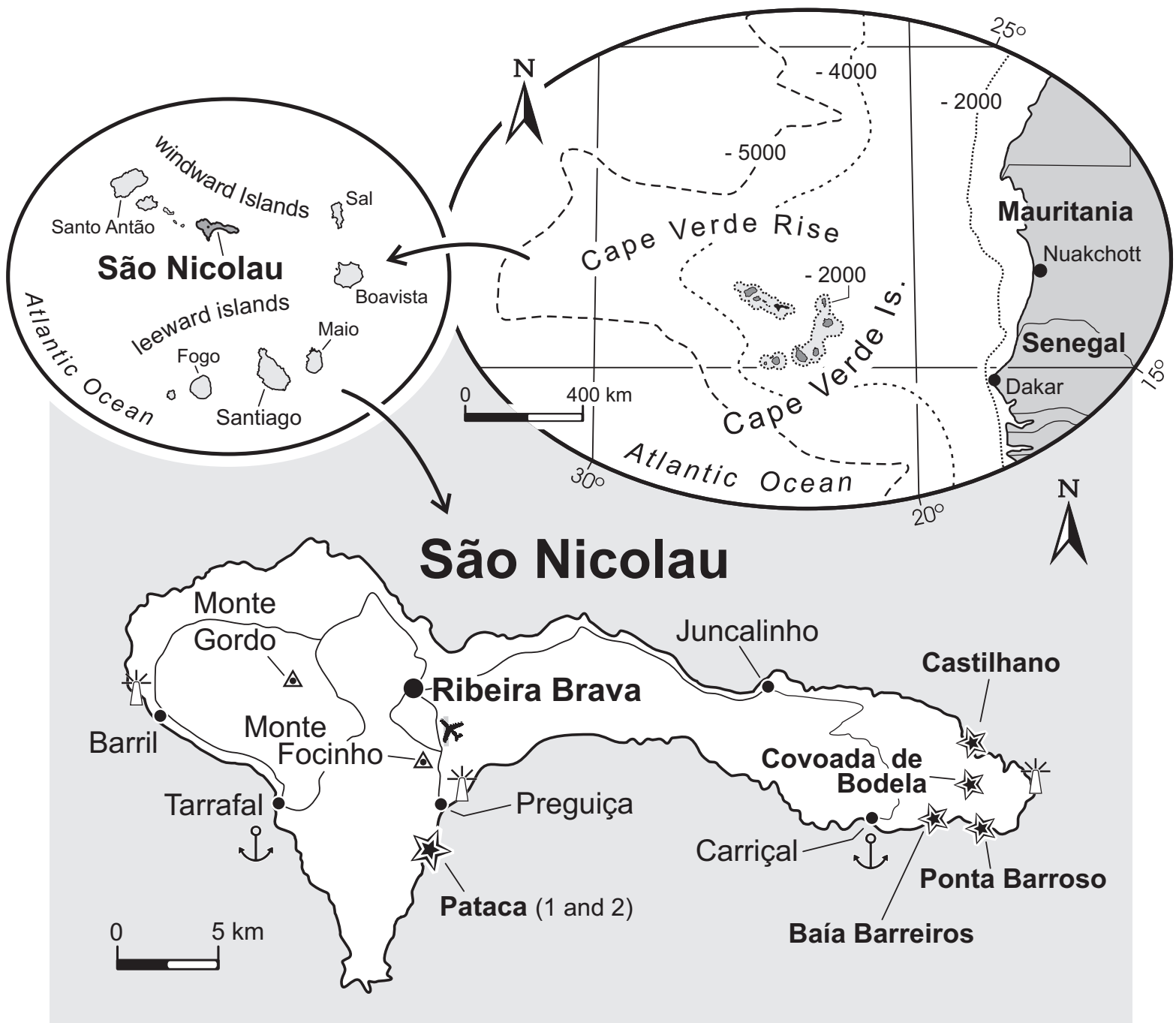


Figure 2

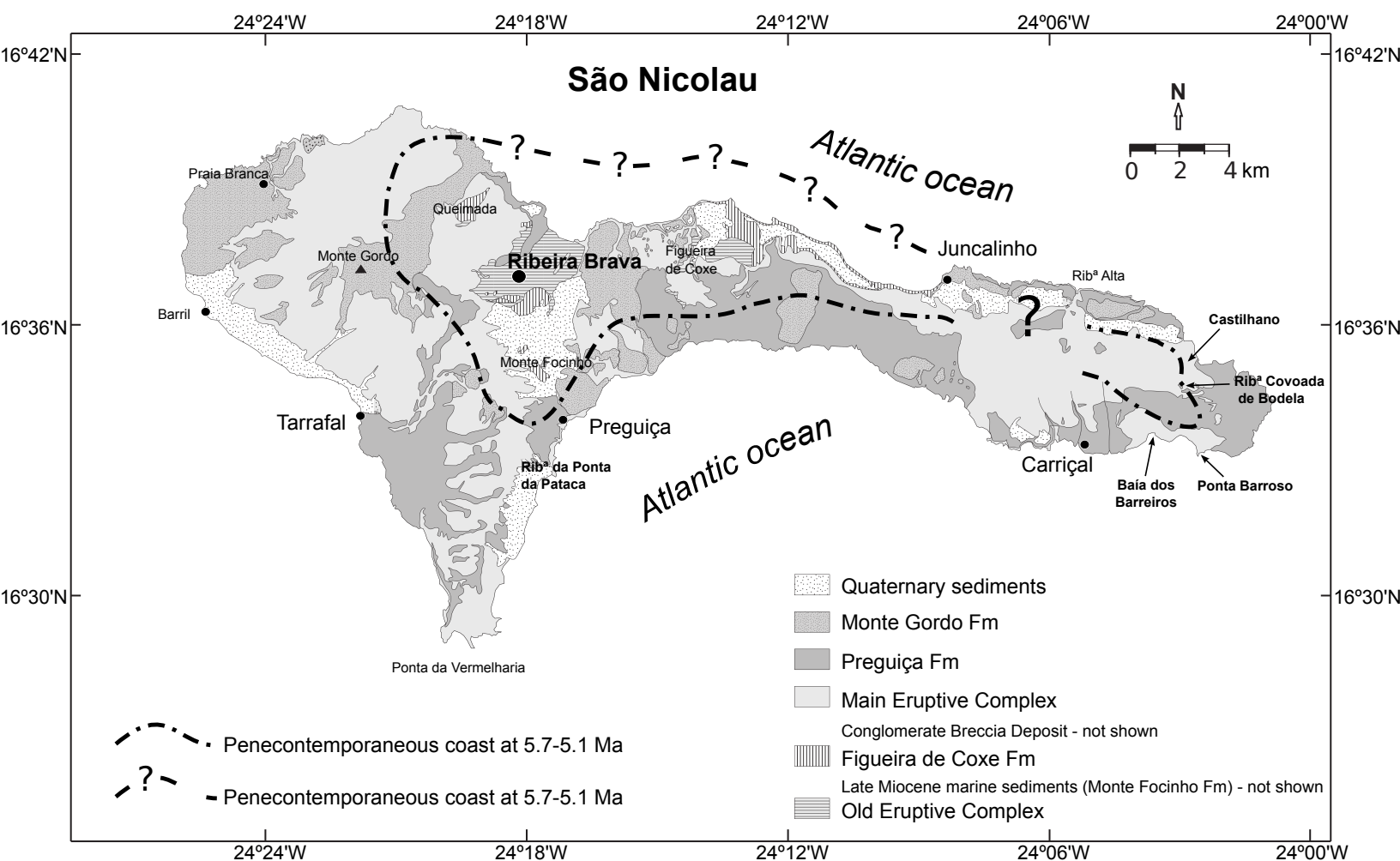


Figure 3

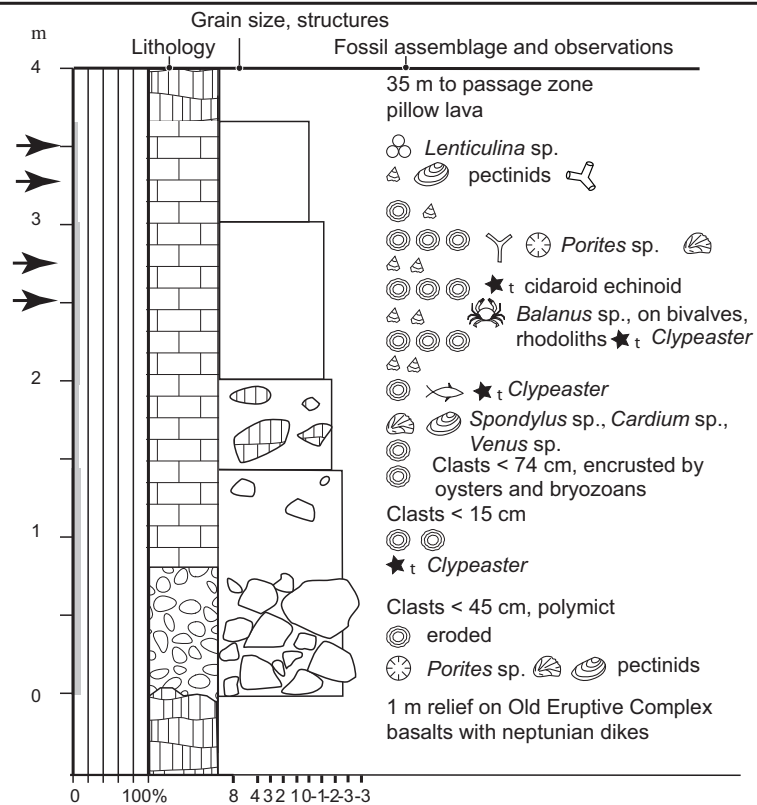
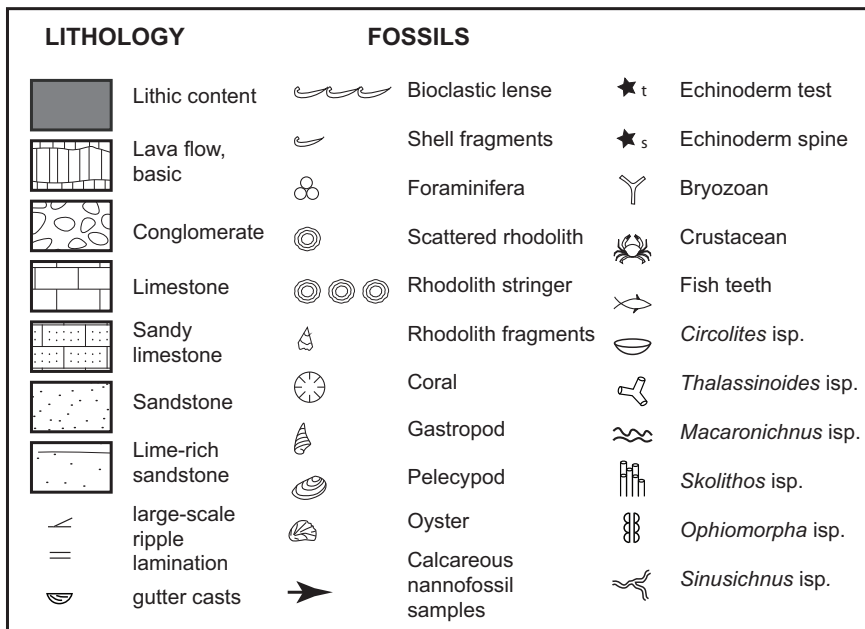
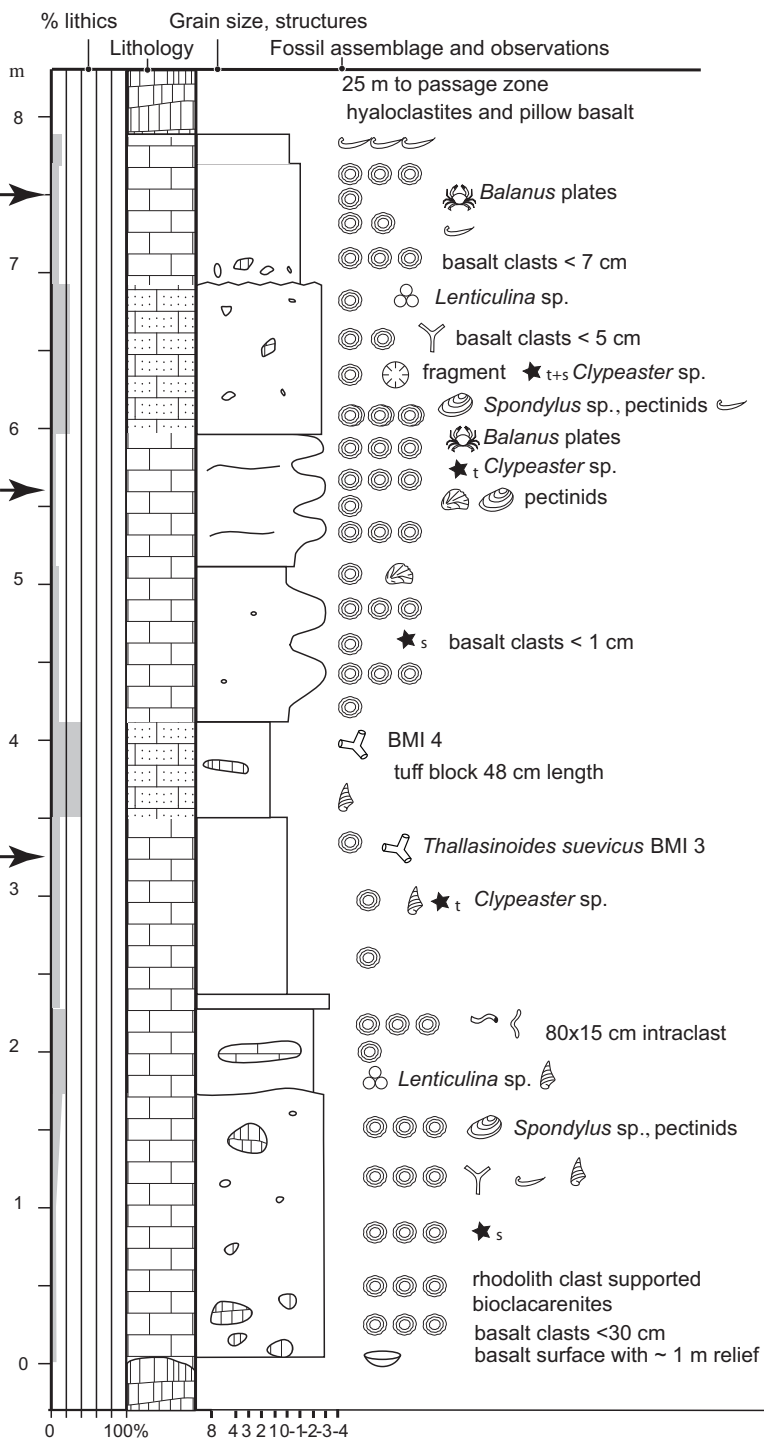
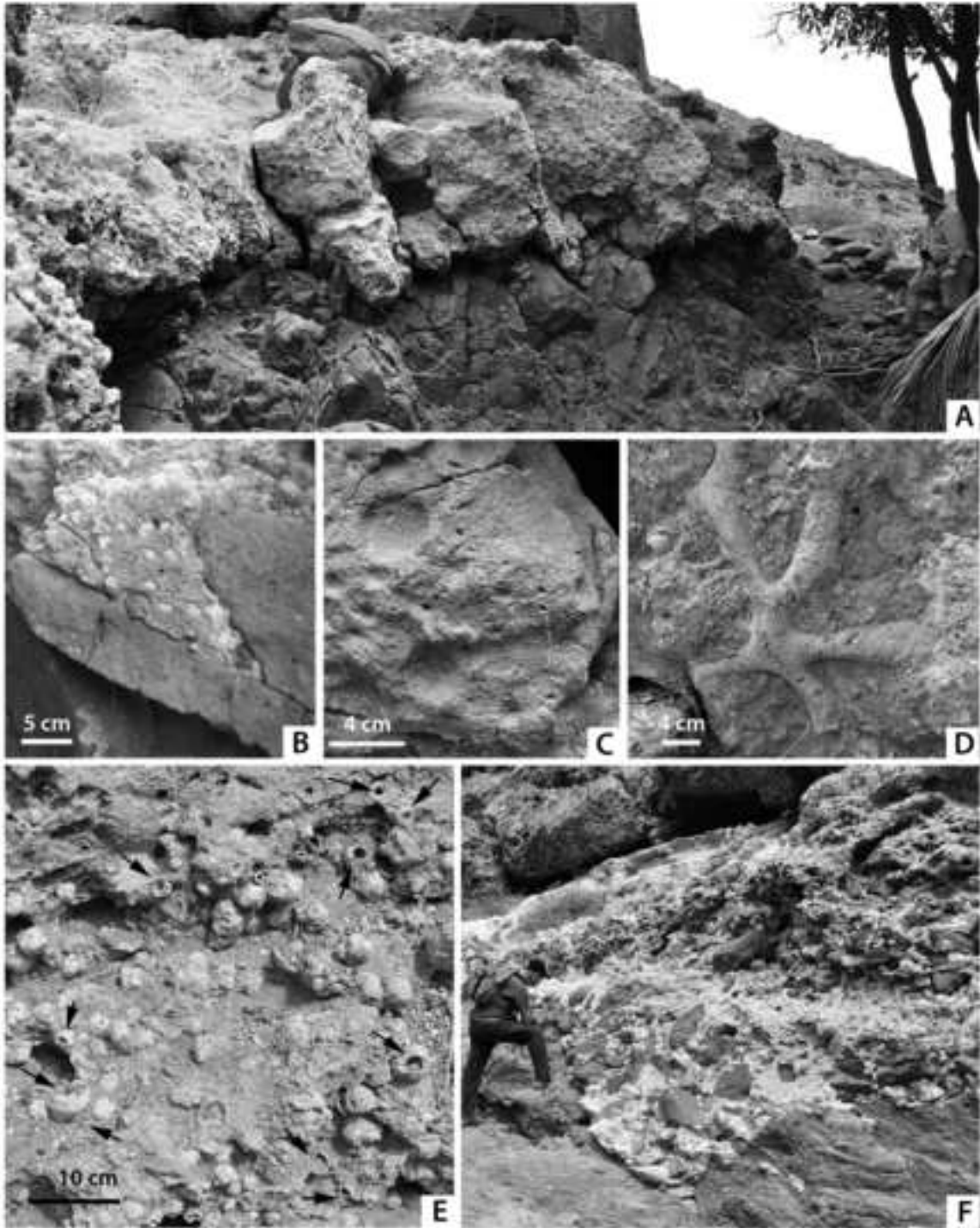


Figure 4  
[Click here to download high resolution image](#)



**Figure A5**

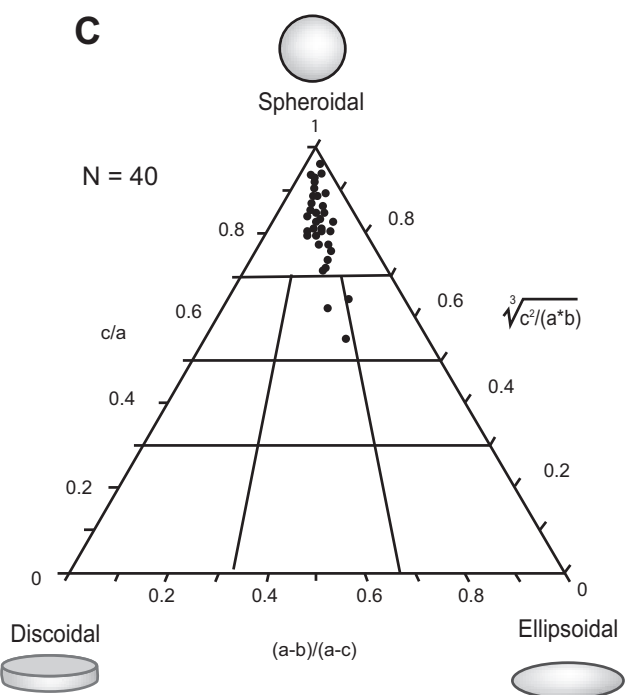
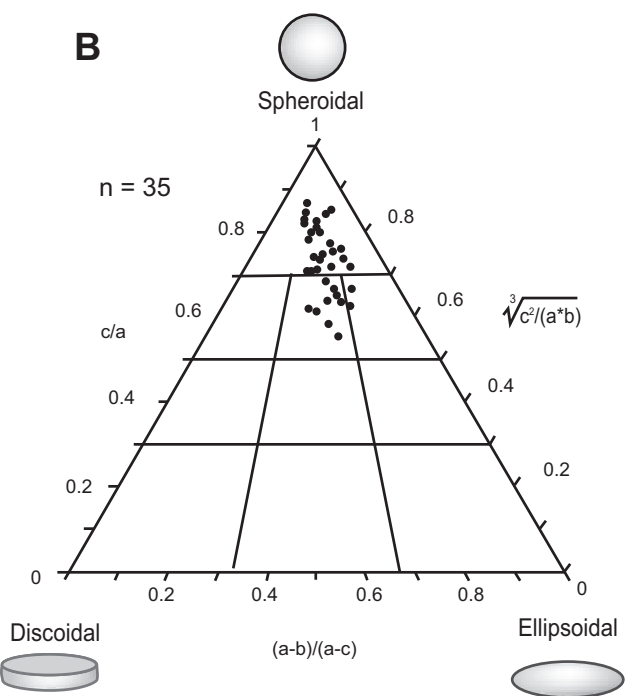
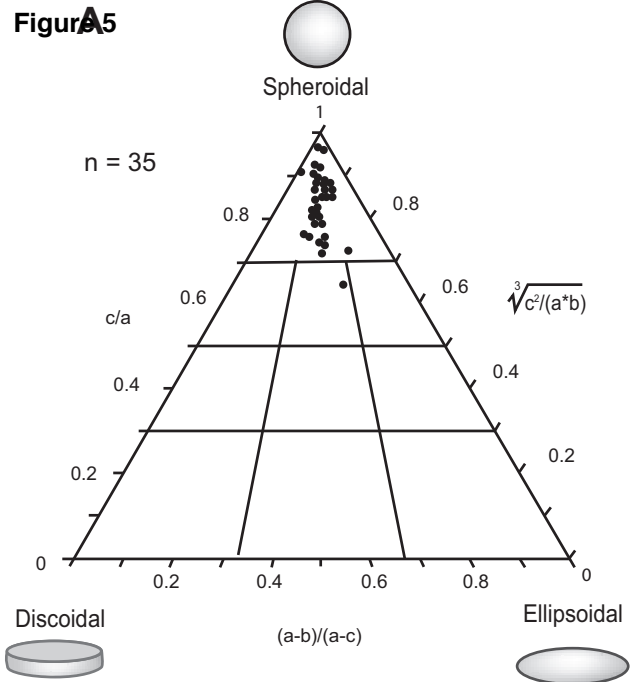
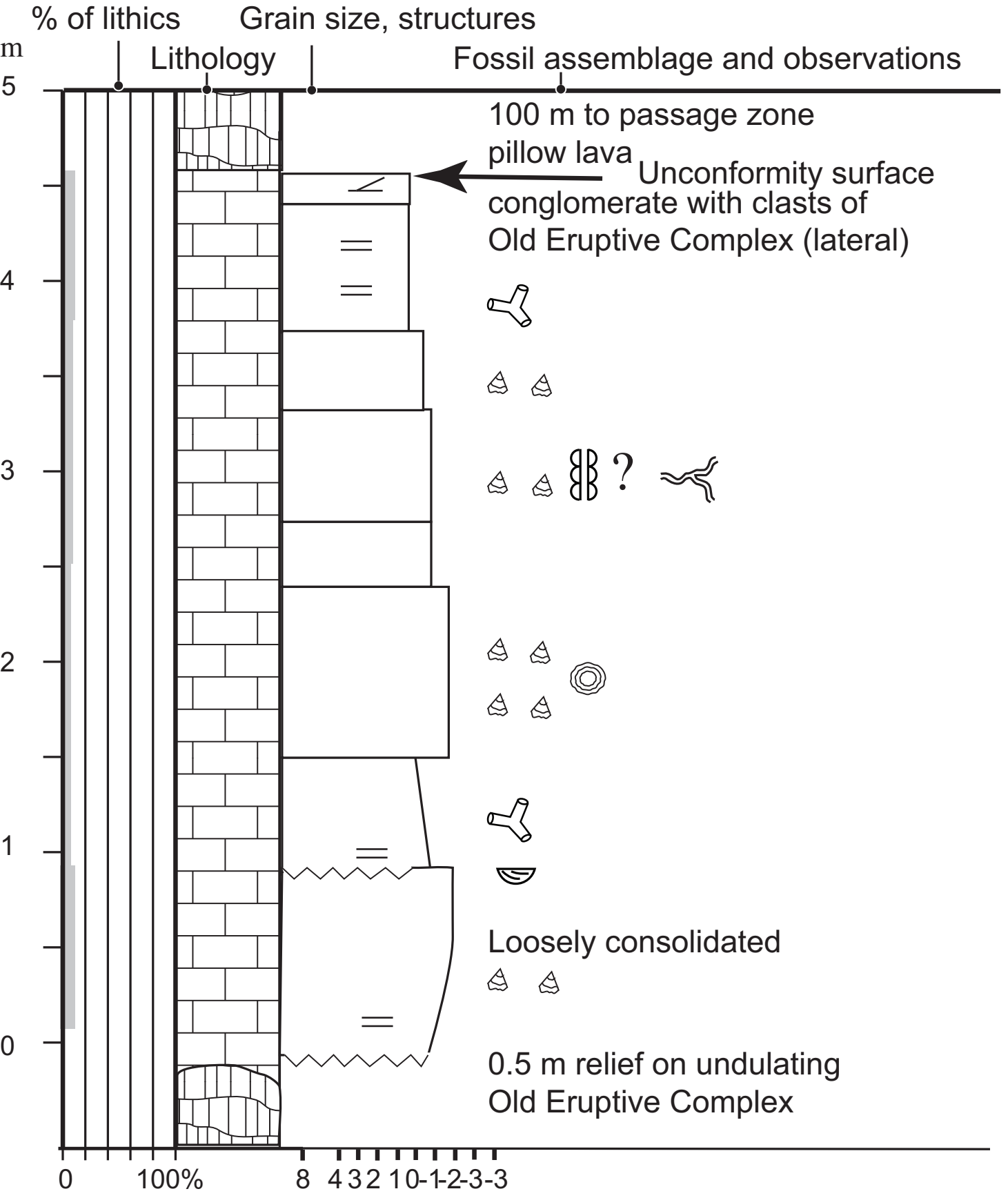
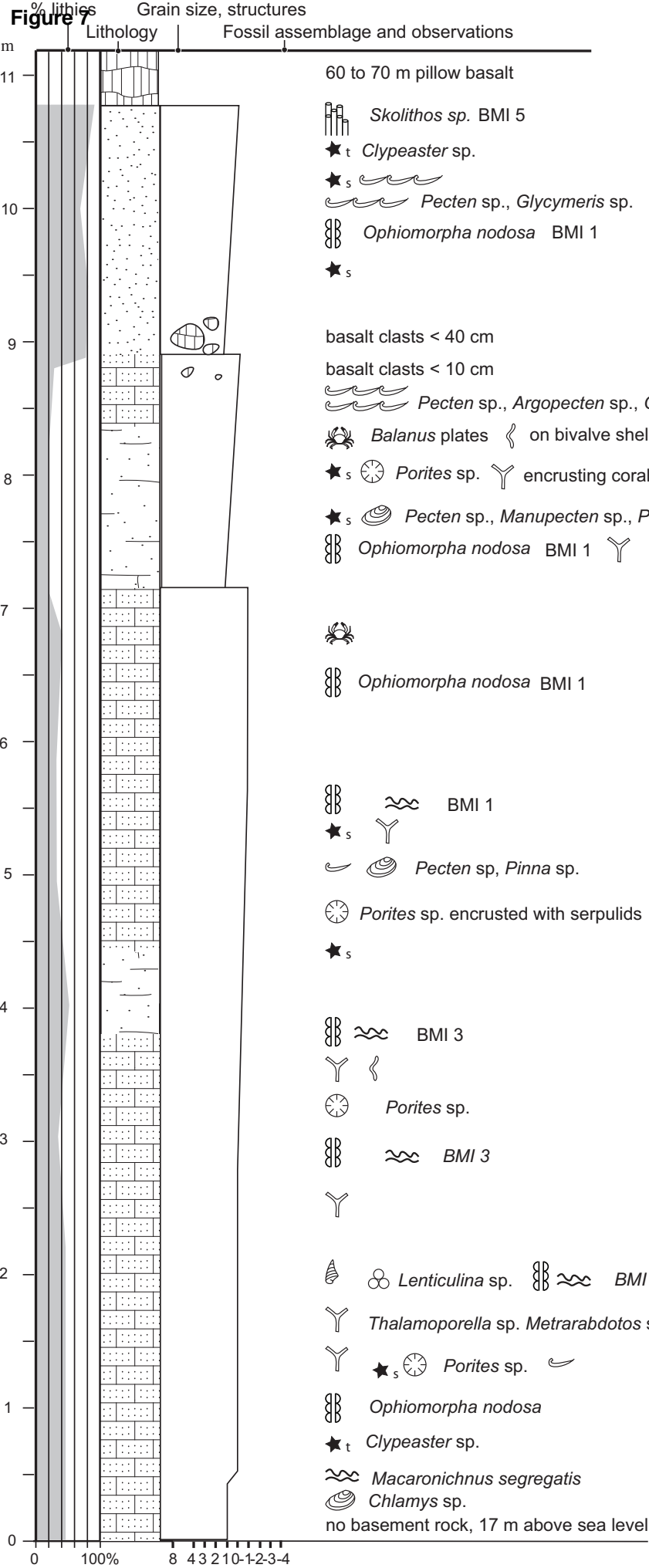


Figure 6



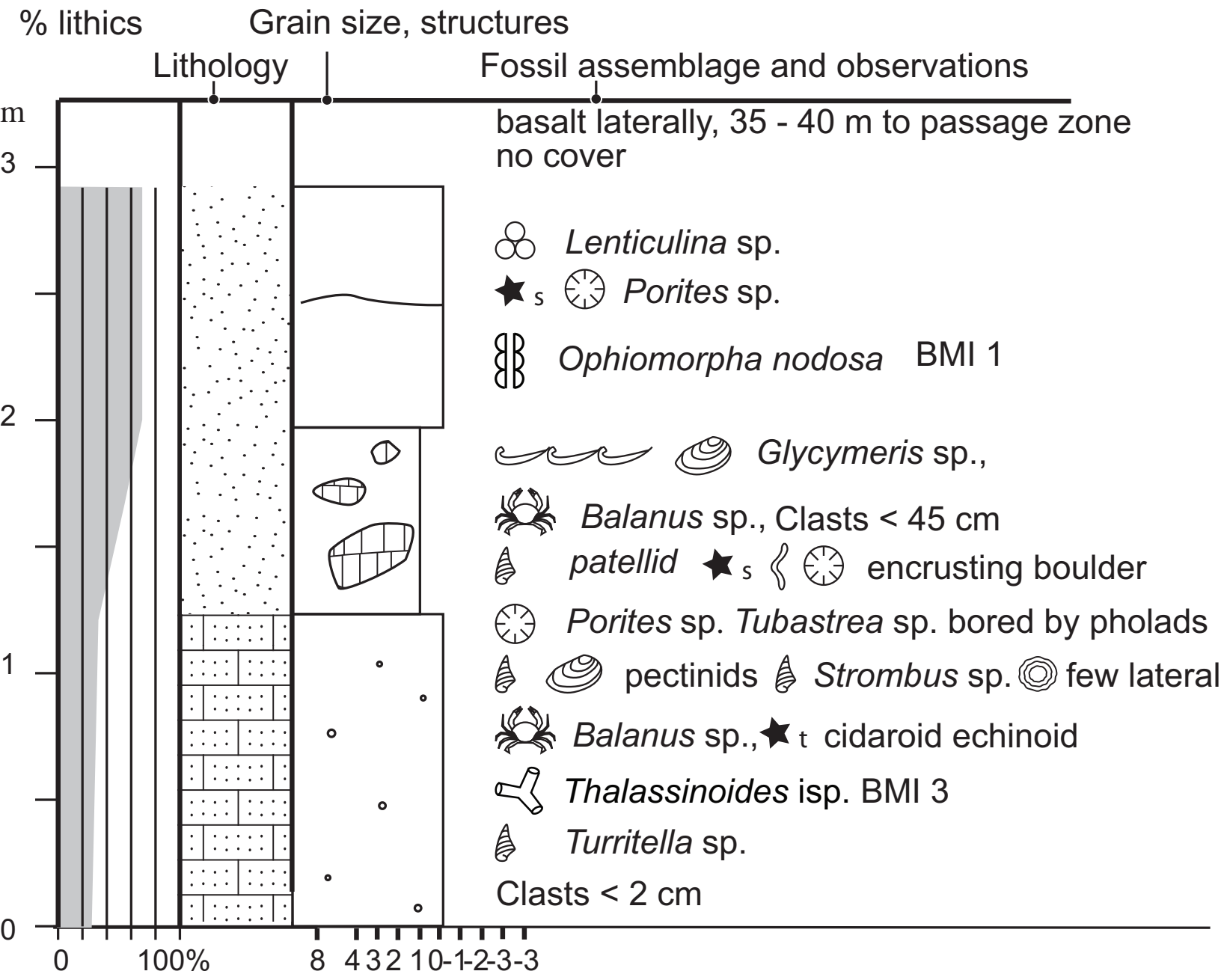
# Barreiros





Pataca 1

Figure 8



Pataca 2

Figure 9  
[Click here to download high resolution image](#)

